CZECH UNIVERSITY OF LIFE SCIENCES PRAGUE

FACULTY OF ENVIRONMENTAL SCIENCES

The isotopic fractionation of cadmium during adsorption on goethite and ferrihydrite

DIPLOMA THESIS

Mammadov Bakhtiyar

THESIS SUPERVISOR: Ing. Zuzana Vaňková, Ph.D.

PRAGUE 2019/2020

CZECH UNIVERSITY OF LIFE SCIENCES PRAGUE

Faculty of Environmental Sciences

DIPLOMA THESIS ASSIGNMENT

Bc. Bakhtiyar Mammadov

Geology

Environmental Geosciences

Thesis title

The isotopic fractionation of cadmium during adsorption on goethite and ferrihydrite

---

Objectives of thesis

The aim of the review part of the study is to summarize basic concepts and knowledge concerning Cd and its occurence in the environment, stable metal isotopes including notation used for their description, adsorption processes, and studies dealing with isotopic fractionation of Cd during adsorption onto various solid phases.

In the experimental part of the thesis, the kinetics and pH-dependence of adsorption of Cd onto two different Fe oxides, ferrihydrite and goethite, will be investigated. The adsorption edges and adsorption kinetics will be visualized graphically and kinetic data will be modelled using the pseudo-second order kinetic equation. For chosen experimental points, Cd isotopic fractionation will be determined using thermal ionization mass spectrometry (TIMS) and compared with the obtained adsorption data.

Methodology

Review part is based on appropriate literature sources, eg., mainly scientific books and articles.

In the experimental part of the thesis, a set of batch adsorption experiments will be performed to evaluate the kinetics and pH dependence of Cd adsorption onto goethite and ferrihydrite. The experiments will be performed under nitrogen atmosphere with initial concentration of Cd set to 10-4 mol/L in a background eletrolyte of 0.1, 0.01 or 0.001 M NaNO3. Data from kinetic experiments will be depicted graphically and modelled using the pseudo-second order kinetic equation. When the adsorption kinetics/adsorption edges will be constructed, chosen points will be analyzed concerning Cd isotopic fractionation before and aGer sorption using thermal ionization mass spectrometry (TIMS). The obtained isotopic fractionation data will be compared with adsorption data and will be further discussed using already published literature.

Obtained data will be processed, summarized and statistically evaluated. Student will discuss the results with existing literature and summarize main conclusions of the work.

The proposed extent of the thesis

Keywords

cadmium; adsorption; isotopic fractionation; ferrihydrite; goethite

---

Recommended information sources

Bryan, A. L., Dong, S., Wilkes, E. B., & Wasylenki, L. E., 2015. Zinc isotope fractionation during adsorption onto Mn oxyhydroxide at low and high ionic strength. Geochim. Cosmochim. Acta 157, 182–197.

Horner, T. J., Rickaby, R. E. M., & Henderson, G. M., 2011. Isotopic fractionation of cadmium into calcite. Earth Planet. Sci. Let. 312(1–2), 243–253.

Wasylenki, L. E., Swihart, J. W., & Romaniello, S. J., 2014. Cadmium isotope fractionation during adsorption to Mn oxyhydroxide at low and high ionic strength. Geochim. Cosmochim Acta 140, 212–226.

Wiederhold, J.G., 2015. Metal Stable Isotope Signatures as Tracers in Environmental. Environ. Sci. Technol. 49, 2606-2624.

Expected date of thesis defence

2020/21 WS – FES

The Diploma Thesis Supervisor

Ing. Zuzana Vaňková, Ph.D.

Supervising department

Department of Environmental Geosciences

Electronic approval: 7. 12. 2020

prof. RNDr. Michael Komárek, Ph.D.

Head of department

Electronic approval: 7. 12. 2020

prof. RNDr. Vladimír Bejček, CSc.

Dean

Declaration

I hereby declare that I have written this diploma thesis titled "*The isotopic fractionation of cadmium during adsorption on goethite and ferrihydrite*" independently under the direction of Zuzana Vaňková. I have listed all literature and publications from which I have acquired information in the reference section.

In Prague, Czech Republic, December 8, 2020

Acknowledgements

I have the deepest gratitude to Ing. Zuzana Vaňková, Ph.D. as my supervisor for her time, support and advice that were very helpful and essential during writing of this Master thesis.

Abstract

The isotopic fractionation can be defined as the distribution of relative amount of heavier and lighter isotopes between the two coexisting phases. This distribution of isotopes can be driven by kinetic or equilibrium effect. The equilibrium isotope fractionation of metals can occur during formation of different complexes due to thermodynamic differences in the bonding environments. It is important to investigate the impact of sorption reactions on the isotopic fractionation of Cd before it can be applied as isotopic signature for the tracing the different environmental processes and sources. The study of Cd isotopic fractionation during sorption on goethite and ferrihydrite was conducted to investigate the difference in isotopic fractionation of Cd at the Fe-oxyhydroxide/water interface. Our result demonstrates that the isotopes of Cd are fractionated during adsorption on goethite and ferrihydrite with the heavier isotope enrichment in aqueous solution. According to our experimental data, we observed predominantly the equilibrium isotopic effect since the fractionation of Cd proceeded through the trend line of isotopic equilibrium. The calculated average equilibrium isotopic fractionation values of Cd during adsorption on goethite and ferrihydrite in aqueous solution were $\Delta^{114/110}Cd_{sorbed\text{-}aqueous}$ = +0.48‰ and $\Delta^{114/110}Cd_{sorbed\text{-}aqueous}$ = +0.18‰, respectively. We hypothesize that the different magnitudes of Cd fractionation in aqueous solution can be associated with the difference in bond valence of Cd-O and different complexation mechanisms that could be driven by coordination chemistry of originating metal complexes. The presented results need further investigation since we did not provide the directly measured data on isotopic fractionation of Cd on studied minerals. The data from EXAFS analyses (currently under preparation) could also further elucidate the relations between the measured adsorption and isotopic data and explain more the complexation processes involved.

Key words: cadmium; adsorption; isotopic fractionation; ferrihydrite; goethite

Table of Contents

1. Introduction

Stable isotope analysis of heavy and light chemical elements is used and applied in various scientific fields for comprehending the biogeochemical cycling of metals, environmental tracing, evolution of the Earth, identifying the sources of ore-forming materials, isotopic fractionation etc. (White, 2004; Wiederhold, 2015). Due to the improvements in advanced instrumentation and techniques such as Multi-Collector Inductively Coupled Plasma Mass Spectrometry (MC-ICPMS) and Thermal Ionization Mass Spectrometry (TIMS), we have the opportunities to study non-traditional stable isotopes fractionation in anthropogenic and natural materials, which include stable isotopes of Li, Fe, Cd, Cu, Zn, Mo and Ge (Chuanwei, 2015). Among these chemical elements, Cd shows toxicity and detrimental impact on environmental systems and substitution with other metals in rocks, such as Zn. According to the Goldschmidt classification and from the geochemical point of view, Cd has volatile behavior in cosmo-chemical or geological processes. As mentioned in Lockington et al. (2014), Cd exhibits siderophilic properties similarly as Zn and due to their similar geochemical behavior, ionization potential, and comparable electron structure, Cd is mostly associated with Zn minerals (sphalerite, wurtzite etc.) and is also able to substitute Zn atoms in crystalline lattice of minerals. It also has lithophilic behavior, which means this element is associated with carbonate sediments and can be a valuable evidence of strong latitudinal and vertical Cd isotopic fractionation variations in past seawater or ocean regions due to biological uptake (Chuanwei, 2015; Horner et al., 2010; Lacan et al., 2006; Wasylenki et al., 2014). The exploration Cd isotope composition and fractionation mechanism can be also applied as the tool for the understanding of ore genesis of Pb-Zn deposits (Zhu et al., 2013).

In these latter years, the adsorption of Cd onto Fe and Mn oxides, which could be associated with a distinctive isotope effect has been widely studied. One of the examples could be related to the battery production, when Cd as the one of the toxic metals tends to end up in shallow aquifers. In this environment, Cd does not change the oxidation state, so its mobility is influenced mainly by adsorption. In comparison with clays and other silicates, the oxides and hydro-oxides of Mn and Fe are more effective in terms of adsorption. The advantage of Fe and Mn oxides is the high surface area and strong affinity of metals to adsorbent at near neutral pH conditions. If the adsorption process of Cd to

these minerals could be related to the distinctive isotope effect, then in this case the adsorption and fractionation of Cd isotopes in the form of the flow of dissolved Cd through polluted aquifer would be seen in a pattern of isotope variability (Wasylenki et al., 2014).

The studies of Cd isotopes in terms of understanding the dependence of isotopic fractionation on adsorption mechanism or vice-versa in comparison with other metal stable isotopes is still at an exploratory stage.

2. Aims of the thesis

The main objective of this thesis is to provide the data on Cd isotopic fractionation during the adsorption onto two Fe oxyhydroxides, ferrihydrite and goethite. Firstly, the kinetics and pH-dependence of adsorption of Cd onto these two phases will be investigated. The adsorption edges and adsorption kinetics will be visualized graphically and kinetic data will be modelled using the pseudo-second order kinetic equation. For chosen experimental points, Cd isotopic fractionation will be determined using thermal ionization mass spectrometry (TIMS) and compared with the obtained adsorption data.

3. Literature Review

3.1 Isotopes – an overview

Isotopes are atoms with the equivalent number of protons and electrons, but a different number of neutrons. Isotopes can be formally described as ${}^{M}_{Z}\mathrm{X}$,where X stands for any chemical element. The number M is the atomic mass of the element, which is equal to the sum of protons and neutrons; the number Z stands for the atomic number, which is the equivalent to that of protons. The number of neutrons for all elements can be determined by the difference of the atomic mass and number of protons. The word "isotopes" in Greek means "equal places", which means that they occupy the same position in the periodic table due to their identical atomic numbers (Tiwari et al., 2015). Isotopes that spontaneously decay with a measurable half-life are called radioactive, whereas those that do not decay or have an extremely long half-life, almost the same as the age of the Earth, are considered as stable isotopes (Wiederhold, 2015).

Most chemical elements have several natural isotopes due to the reason that the variable number of neutrons is able to form stable and long-lived nucleus and the relative abundance of these isotopes can be also extremely different. Most elements have isotopes that contains neutrons in quantity that makes them unstable. Although most isotopes have an extremely short half-life and are only visible in artificial conditions (> 80% of 2500 nuclides), many of them are produced by naturally occurring processes and have a long half-life to exist in the environment in measurable quantities. These processes include: decay of the parent isotopes, nuclear reactions, nuclear explosions, reactions taking place in reactors etc. (Baskaran, 2012). Due to this reason, the produced isotopes are important for the most of methods aiming at obtaining the absolute age and information about environmental processes. The disintegration of isotopes occurs according to the law of radioactive decay, which is considered as random process (Choppin et al., 2002). If we denote the decay rate by A (Equation 1), and take into the account the number of the disintegrations per unit of time, it will be expressed as mentioned below:

$$A = -dN / dt \qquad \text{Equation 1}$$

3.2 Stable Isotopes

There were several scientific fields, such as chemistry, geochemistry, biochemistry and ecology, where the stable isotope analysis was applied as a unique tool for sourcing, identification, tracing and recording different processes and changes in Earth's various environmental systems (Hoefs, 1997).

In contrast to radioactive isotopes, stable isotopes are not able to decay. Moreover, these isotopes can be treated as the energetically stable ones. The stable isotopes can be considered as stable, when the ratio of the neutrons (N) and protons (Z) is less or equal to 1,5 ($N/Z \leq 1{,}5$; Figure 1) (Michener & Lajtha, 2008). In general, there are almost 1200 radioactive isotopes, 300 stable isotopes, and only 21 elements have only one isotope (Hoefs, 1997).

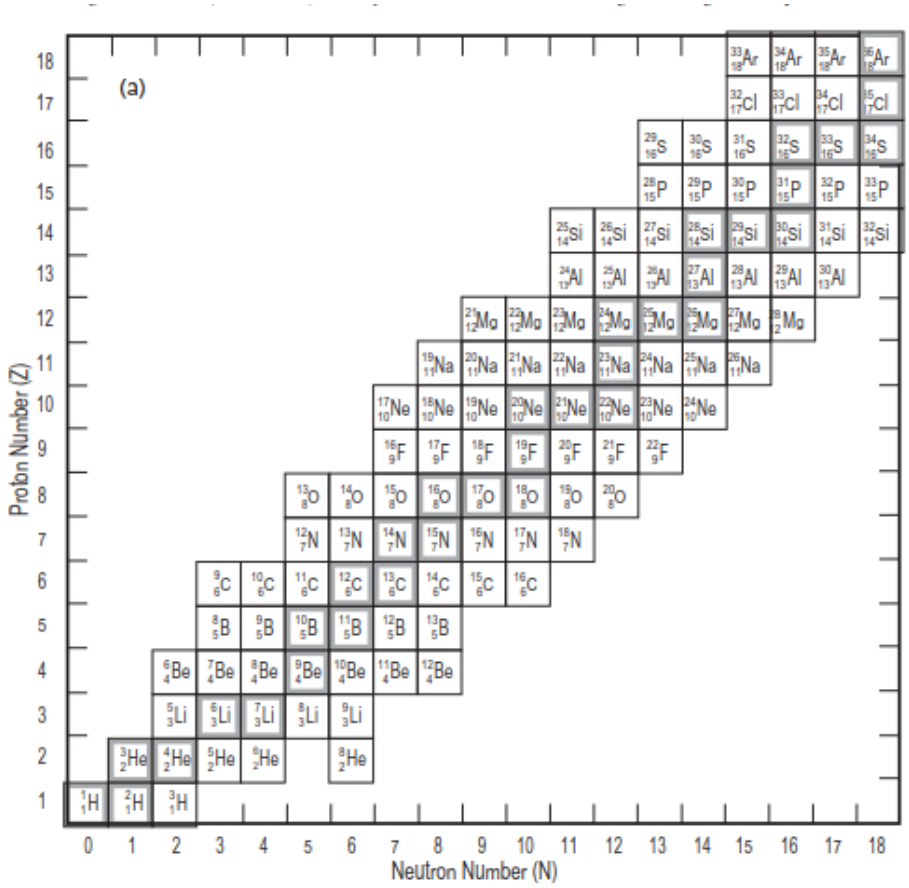

Figure 1 (a)- the periodic table of the lighter unstable and stable isotopes. Shaded borders indicate stable isotopes and unshaded ones depict short-lived unstable isotopes; adapted from Michener & Lajtha (2008)

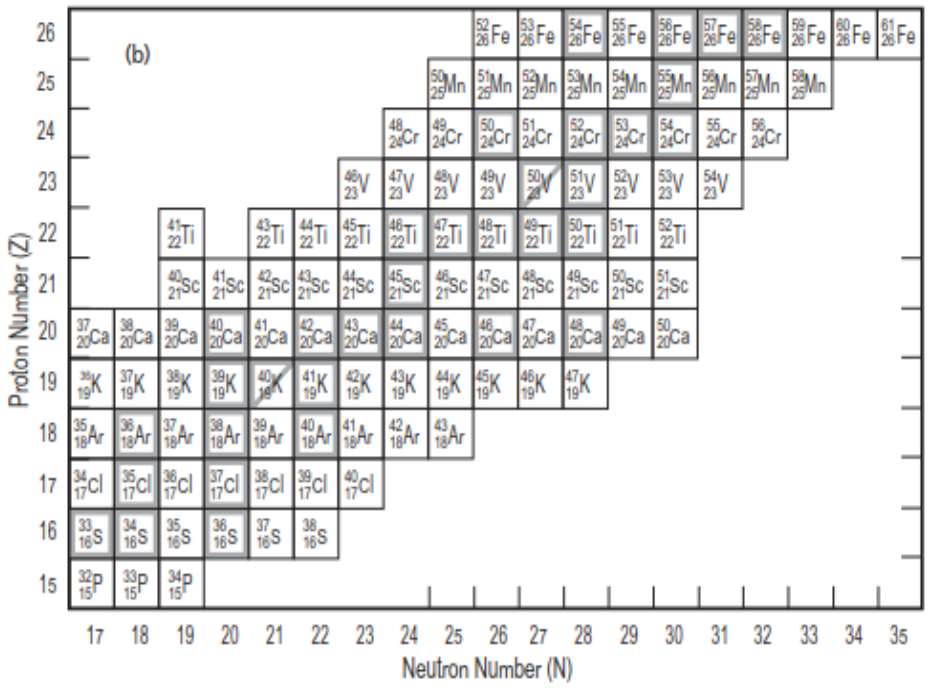

Continuing -(b)- the periodic table of the heavier unstable and stable isotopes. Shaded borders indicate stable isotopes and unshaded ones depict short-lived unstable isotopes. Long-lived unstable isotopes are highlighted with a triangular border (^{40}K).

3.3 Isotopic fractionation, fractionation factor and delta value

Isotope fractionation is determined by the relative distribution of the heavier and lighter isotopes between 2 coexisting phases and can occur due to kinetic or equilibrium effects (Tiwari et al., 2015).

Equilibrium fractionation is a distribution of isotopes between 2 coexisting phases without any net reaction, being the special case of chemical equilibrium reaction, affecting also the equilibrium constant. In this case, isotopes can move back and forth until equilibrium is achieved, and when it is attained, the isotopic ratios do not change more over time. For example, as foraminifera (a unicellular microorganisms) set off their calcite shells in equilibrium with the surrounding sea water, and it is followed by the occurrence of isotopic exchange process:

$$1/3CaC^{16}O_3 + H_2{}^{18}O \rightleftharpoons 1/3CaC^{18}O_3 + H_2{}^{16}O$$

where," K" – the equilibrium constant can be expressed as:

$$K = \frac{[CaC^{18}O_3]^{1/3}\ [H_2O^{16}]}{[CaC^{16}O_3]^{1/3}\ \ [H_2O^{18}]}$$

Therefore, equilibrium constant can be determined as the ratio of $^{18}O/^{16}O$ in the carbonate phase to that in the water. This leads to the concept of isotopic fractionation factor "α", which means the distribution of isotopes between two phases (Tiwari et al., 2015). As can be seen from the Equation 2, the ratio of isotopes between two compounds is often defined as the fractionation factor alpha (α) (Wiederhold, 2015).

$$\alpha_{A-B} = \frac{R_X}{R_Y} \qquad \text{Equation 2}$$

where, R_X and R_Y are the ratios of isotopes of element R in phases X and Y.

In the $CaCO_3$–H_2O system, the fractionation factor is expressed as:

$$\alpha_{CaCO_3-H_2O} = \frac{\left(O^{18}/O^{16}\right)_{CaCO_3}}{\left(O^{18}/O^{16}\right)_{H_2O}}$$

The fractionation factor (α) is also associated with equlibrium constant and can be determined by the formula below (Equation 3) (Tiwari et al., 2015):

$$\alpha = K^{1/n} \qquad \text{Equation 3}$$

"n" – is the number of exchanged atoms.

Since we discussed the isotopic ratio of $^{18}O/^{16}O$ in the carbonate phase to that in the water, it will be crucial to explain the meaning of delta value for isotopic ratio. One of the most difficult issues is the precise measurement of the absolute isotope ratio due to the extremely low amount of the heavier isotopes. According to this, the isotope ratio is determined by the ratio of the number of the heavier to lighter isotopes. In Wiederhold (2015) provided the definition that the isotopic variations and changes are expressed as delta values "δ" by indicating the ratio of isotopes in sample to the ration of isotopes in standard materials (Equation 4):

$$\boldsymbol{\delta_A} = \left[\frac{(E^x|E^y)_{\text{sample}}}{(E^x|E^y)_{\text{standard}}} - 1\right] \qquad \text{Equation 4}$$

where x and y represent isotopes of the element E. The delta (δ) value is very low and unitless. Due to this reason, this value is usually multiplied by the factor of 10^3, when it can be expressed in "per mil "(‰) units (Tiwari et al., 2015; White, 2004).

Before going to explain the process of kinetic fractionation, it is important to start with the reactivity of isotopes and their compounds. The chemical reaction is controlled by the number of the atom's outer shell electrons; this is the reason of qualitative similarity of chemical behavior of 2 isotopes.

But it is important to point out that the isotopes have different mass and the differences in atomic mass can influence the bond strength and reaction speed. The most significant differences specifically can be seen in lighter elements, where the mass difference is the highest. For instance, the deuterium atom has a double mass of the hydrogen atom, meanwhile the additional neutron in ^{33}S is only a 3 % increase in mass over ^{32}S. Due to this reason the behavioral differences between hydrogen and deuterium will be much larger those between ^{33}S and ^{32}S. This mass differences can be a result of physical behavior differences due to the reason that the kinetic energy (KE) is stable for a certain element (Equation 5a, b) (Michener & Lajtha, 2008):

a) $\mathrm{KE} = \frac{1}{2}\mathrm{mv}^2$ b) $\frac{v_L}{v_H} = \sqrt{\frac{m_H}{m_L}}$ Equation 5a, b

where, mass of heavier and lighter isotopes is expressed with m_H and m_L , respectively, and velocity of heavier and lighter isotopes is signed with v_H and v_L. By the simple formula, we are able to see that the different masses of the same molecule react with the different rates, where L and H mean lighter and heavier isotopes. For example, $[H_2O^{16}]$ and $[H_2O^{18}]$.

$$\frac{v_L}{v_H} = \sqrt{\frac{20}{18}} \qquad \text{Equation 6}$$

As can be seen from the Equation 6, the velocity of $[H_2O^{16}]$ is 1.05 times higher than that of $[H_2O^{18}]$.

In general, kinetic fractionation is usually associated with fast, incomplete, or unidirectional processes, such as evaporation, diffusion, and dissociation reactions (White, 2004). Kinetic isotope effects occurs due to the difference between reaction rates of light and heavy isotopes. The impact of kinetic effects on the isotopic composition of sample is strongly associated with the relative degree of reaction progress. The highest kinetic isotope effect can be observed from remaining reactants, when the reaction is far from completion since the reactants are strongly enriched with heavy isotopes and continuously removes the lighter isotopes. If the reaction will be completed and all reactants transformed to the products, then the signature of kinetic effect can be erased since the isotopic ratios of products will be the same as the initial reactants.

The difference of kinetic and equilibrium isotopic effects can be seen from Figure 2. Both types of fractionation can affect natural samples, and it is often difficult to figure out their relative control on the observed metallic stable isotopic signatures. The main difference of kinetic fractionation (Figure 2a) from equilibrium isotopic effect is that it can be driven by the speed of particles during e.g., diffusion, meanwhile the equilibrium effect is determined by the stiffness of originating bond. Equilibrium isotope effects (Figure 2b) are caused due to the forward and backward reactions between 2 coexisting phases proceeding at equal rates. Consequently, the differences of energy in bonding environments of reaction partners controls the relative isotopic abundance which have reached isotopic equilibrium. However, there is difference in time scale between isotopic equilibrium and concentration equilibrium, the concentration equilibrium can take some minutes, but equilibrium isotopic effect can last some days or even years. When isotopic equilibrium occurs, then heavy isotopes are enriched in “stronger bonding environments”. This environment can be in metal species with lower coordination number or due to shorter bond length in present complexes. This can be explained by the lower zero-point energies of bonds in molecules with heavy isotopes as compared to bonds with light isotopes of the same element (Wiederhold, 2015).

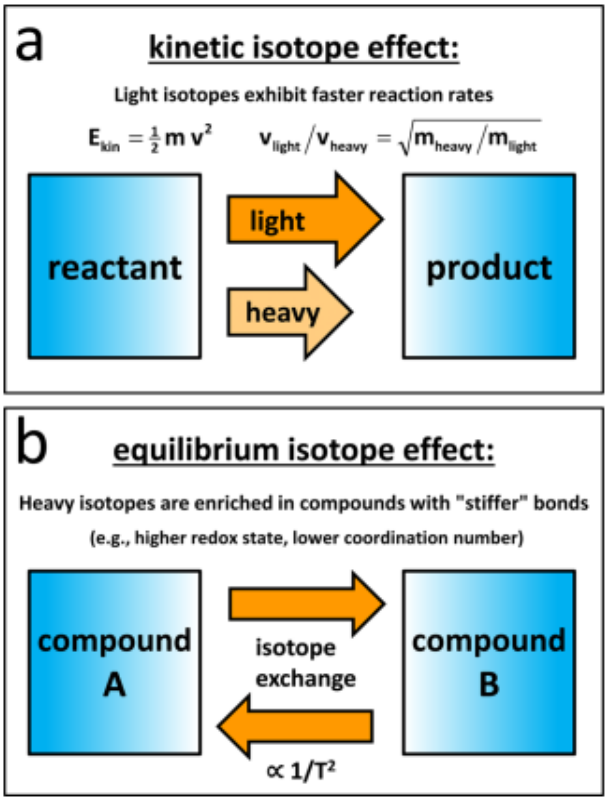

Figure 2 The schemes of kinetic (a) and equilibrium (b) stable isotope fractionation (Wiederhold, 2015).

3.4 The characteristics and geochemical occurrence of Cd

Cadmium is a lustrous, bluish white and soft metal with ecotoxic properties, which was discovered in 1817 by Friedrich Strohmeyer of Gottingen during Cd-rich Zn-oxide or carbonate analyzing procedure. Cadmium has eight stable or quasi-stable isotopes, which vary in mass number from 106 to 116. It was discovered in 1930s by mass spectrometric analyses of Astron, Nier and others (Rehk, 2013). The significant natural source of Cd isotope variations are stable isotope fractionations. The isotopes ^{113}Cd and ^{116}Cd are long-lived radio-active isotopes that transform to ^{113}In and ^{116}Sn by β^-decay (Pfennig, 1998). The values of the physical and chemical properties of Cd can be seen from Table 1.

Table 1 The physo-chemical properties of Cd; adapted according to Rehk (2013).

Property	
Atomic Number	48
Standart atomic weight (g/mol)	112.411
Electron configuration of Cd°	[Kr] $4d^{10}$ $5s^2$
Melting point (°C)	320.9
Boiling point (°C)	767.3
Density of solid at 25°C (g/cm³)	8.642
Density of liquid at m.p. (g/cm³)	8.02
Oxidation states	2; +1 (rare)
Electronegativity[a]	1.69
E^o for $Cd^{2+} + 2e^- = Cd$(V)	-0.402
First ionization energy (kJ/mpl)	867
Second ionization energy (kJ/mol)	1 625
Atomic radius (pm)	155
Ionic radius of Cd^{2+} (pm)	95
Mohrs hardness	2,0

In nature, Cd is mostly associated with Zn, but it has also a strong affinity to S. Additionally, Cd minerals such as greenockite (CdS) and otavite ($CdCO_3$) are found together with Zn minerals, which are also associated with S and CO_3 groups (Kabata-Pendias & Pendias, 2001). Cadmium can be found in association with Pb and Zn minerals such as galenite and sphalerite, due to this reason it is also considered as the by-product of metallurgical processing of Pb and Zn ores. As mentioned above, the most common mineral of Cd is greenockite (CdS), which can react with ammonia and cyanide and form complexes and hydroxides. Cadmium has low melting point (321 °C) and boiling point (765 °C). The Cd compounds are able to vaporize easily in Pb-Zn smelter or coal-fired power plants due to high temperature processes, which can result in anthropogenic contribution to Cd emissions. Hence, the comprehension to Cd isotopic variations during these processes is crucial. The evidence of Cd isotopes in sulfide-rich deposits have been reported by several studies (Shiel, 2010; Schimtt, 2009; Wen, 2015)

The amount of Cd in sedimentary and igneous rocks is approximately 0.3 ppm, and commonly can be found in composition of the carbonaceous shale deposits (Kabata-Pendias & Pendias, 2001). The distribution of the concentration of Cd varies in different ecosystems, as can be seen from Table 2.

Table 2 The concentration (ppm) of Cd in different environmental media; adapted from Adriano (2001)

Material	Avarage concentration	Range
Igneous rocks	0.082	0.001-0.60
Metamorphic rocks	0.06	0.005-0.87
Sedimentary rocks	3.42	0.05-500
Recent sediments	0.53	0.02-6.2
Crude oil	0.008	0.0003-0.027
Coal	0.1	0.07-0.18
Fly ash	11.7	6.5-17
Phosphate rocks	25	0.2-340
Phosphated fertilizers(mixed)	4.3	1.5-9.7
Sewage sludges	74	2-1100
Soils (world nonpolluted)	0.35	0.01-2.0
Australia		
Fertilized rural soils	0.42	0.01-13.9
Unfertilized soils	0.37	0.01-12.02
U.S soils (national arable, n=3202)	0.255	0.03-0.94
Fruits (USA, n=190)	0.005	0.0043-0.012
Vegetables (USA, n=1891)	0.028	0.016-0.13
Crop gains (field-USA, n=1302)	0.047	0.014-0.21
Field crops (USA, n=2858)	0.21	<0.001-3.80
River sediments (polluted)	—	30 ->800
River sediments (unpolluted)	—	0.04-0.8
Grasses	—	0.03-0.3
Ferns	0.13	—
Mosses	—	0.7-1.2
Lichens	—	0.1-0.4
Trees, deciduous		
Leaves	—	0.1-2.4
Branches	—	0.1-1.3

3.5 Sorption Phenomena

3.5.1 Introduction and terminology

Sorption reactions on both organic and inorganic particulates play a key role in controlling the fate and migration of many trace elements in environmental systems. The word “sorption” is referred as the removal of a solute from solution to a solid phase (Smith, 1999). Before going further to details, it will be better to define several terms about the retention (adsorption/sorption) of molecules and ions in soil. Sorption is recognized as the general term, which may encompass adsorption, absorption, surface precipitation, coprecipitation and diffusion into the solid phase. “Sorbate” and “adsorbate” is defined as the solute that accumulates or sorbs on solid phase, while “adsorbent” and “sorbent” means the solid phase onto which the solutes and the molecule

or ion sorbs. Adsorption is one of the most widely used physico-chemical process for removing pollutants from contaminated aqueous media. Adsorption is a significantly time dependent chemical process, which is defined as the two-dimensional accumulation of substances at solid phase. Meanwhile, surface precipitation is considered as the three-dimensional accumulation processes, but adsorption does not comprise of surface precipitation. Both of them are sorption processes, which can be used as the general term when the retention mechanism at the surface is not clear (Smernik, 2003; Smith, 1999). The adsorption depends on the existence of a force field at the surface of a solid, which involves both physical and chemical forces. The physical adsorption includes dispersion-repulsion forces (Van der Waals forces) or Coulomb attraction between sorbate and surface ion, which are supplemented by electrostatic outer-sphere complexation. In the case of physical adsorption, the sorption processes are controlled by the minerals' surface charge (Ruthven, 2008; Smith, 1999). Meanwhile, the chemisorption consists of a significant degree of transfer or exchange of electrons between sorbent and adsorbate, which results in inner-sphere complexation that also involves hydrogen, covalent and ligand exchange mechanism (Ruthven, 2008; Smernik, 2003). The chemical forces are much stronger and the adsorption energies are significantly greater than those for physical one, as can be seen from the Table 3.

Table 3 Physical adsorption and chemisorption; adapted according to Ruthven (2020).

Physical adsorption	Chemisorption
Low heat of adsorption (1.0 to 1.5 times latent heat of evaporation)	High heat of adsorption (>1.5 times latent heat of evaporation)
Nonspecific	Highly specific
Nonspecific	Monolayer only
No dissociation of adsorbed species	May involve dissociation
Only significant at relatively low temperatures	Possible over a wirde range of temperatures
Rapid, nonactivated, reversible	Activated, may be slow and irreversible
No electron transfer, although polarization of sorbate may occur	Electron transfer leading to bond formation betweem sorabte and surface

3.5.2 The principle of adsorption processes of porous adsorbent

As mentioned in previous chapter the adsorption process is the binding of the adsorptive molecules to an adsorbate. The adsorption consists of the mass transfer of species and 3 main steps in case of porous adsorbent as mentioned below. The adsorption processes also can take place on external surfaces of particles in case of non-porous adsorbent. The trajectory of the sorbate molecules/ions to porous adsorbent during adsorption process can be also seen from Figure 3.

Step 1: External diffusion (film diffusion) is the transportation of adsorptive from the bulk phase to the external surface of solid phase.

Step 2: Intraparticle diffusion (pore diffusion) is the transportation of adsorptive from external surface to the internal pore of solid phase.

Step 3: Surface reaction is the attachment of adsorptive molecules to the internal surface of solid phase.

Each step shows the resistance to the adsorbent. Total adsorption rate is determined by overall resistance, which is the sum of three component resistances connected in series. If any component resistance reduces, the adsorption rate increases (Amanullah et al., 2000; Tan & Hameed, 2017).

Among these 3 steps, the third one is taken into account to be the most rapid and poses negligible resistance. The rest two steps provide the following three possibilities:

Possibility 1: External transportation > internal transportation, where the speed of transportation is determined by particle diffusion.

Possibility 2: External transportation < internal transportation, where the speed of transportation is determined by film diffusion.

Possibility 3: External transportation ≈ internal transportation, which takes into account the transfer of adsorbate ions to the boundary and may not be possible at a substantial speed, which later leads to the formation of a liquid film surrounding adsorbent particles with an appropriate concentration gradient (Shanthi et al., 2014).

Adsorption can be studied by two different approaches: equilibrium and kinetic studies. The achievement of equilibrium in adsorptive loading on the adsorbent surface is

governed by thermodynamics. Meanwhile, the adsorption rate depends on the adsorption mechanism. The groundwork for studying kinetics is the kinetic isotherm, which is obtained empirically by tracking the adsorbed amount over time. For better understanding the kinetic studies, various models are developed to explain the rate of adsorption (Tan & Hameed, 2017).

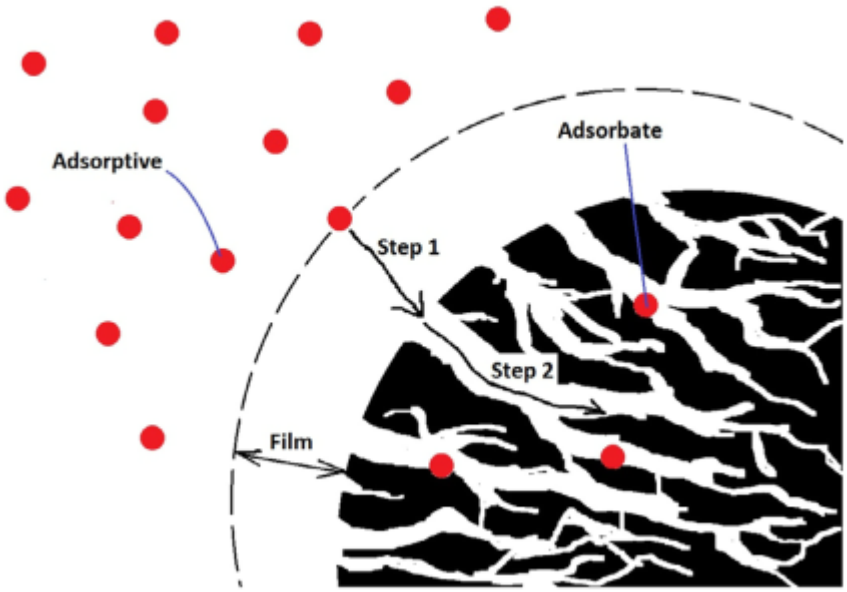

Figure 3 Adsorption of an adsorptive into the internal surface of a porous medium of a solid phase. Step 1 is the film diffusion, and Step 2 is the intraparticle diffusion (Tan & Hameed, 2017)

3.6 Adsorption description

In this subheading, the differences between various types of adsorption description such as adsorption kinetics, adsorption edges, adsorption isotherms, and their application are discussed.

The adsorption kinetic experiments provide the opportunity to determine and describe the adsorption rate and the time needed for achieving the adsorption equilibrium. Adsorption kinetics is a complicated process where diffusion-controlled processes and chemical interactions have their role and influence. The chemical interactions, contribution of desorption processes, film diffusion, and pore diffusion can significantly reduce the adsorption rates and are associated with activation energy. There were done

several attempts in improving and contrasting different kinetic adsorption models, since there is just limited understanding of the theoretical complexity of adsorption mechanism (Bujdák, 2020; Shanthi et al., 2014; Simonin, 2016; Tan & Hameed, 2017).

Before going to the details of the different models applicable for kinetic studies, it will be better to provide some information about the model batch kinetic experiment for modeling the adsorption kinetics. The purpose of this experiment was the film and pore diffusion modelling for adsorption of reactive Red 4 (red dye) onto activated carbon prepared from seed shell waste (Shanthi et al., 2014). This experiment was also performed for the collection of the kinetic data. The batch adsorption studies were conducted at 30 °C. During the batch adsorption, the experimental conditions should be constant. The mixture of known initial concentration of Reactive Red 4 solution and adsorbent (activated carbon) was agitated for certain time. After this, the Reactive Red 4 solution and adsorbent passed through a filter, which separated them from each other. Finally, the residual concentration of Reactive Red 4 in a liquid, which passed through a filter, was spectrophotometrically determined. The adsorbed amount of Reactive Red 4 at time t was determined using the following Equation 7:

$$q_t = (C_o - C_t) \times V / m \qquad \text{Equation 7}$$

where q_t (mg/g) is the adsorbed molar concentration of the adsorptive at time t, C_0 (mg/L) is initial concentration of adsorptive in the bulk liquid at time 0 and C_t (mg/L) is concentration of adsorptive in the bulk liquid at time t, V (L) is the volume of the solution and m(g) mass of the adsorbent (Bujdák, 2020; Shanthi et al., 2014; Tan & Hameed, 2017).

There are two most common empirical models and equations in adsorption studies used to represent the adsorption kinetics: Pseudo-first order (PFO) and pseudo-second order (PSO) model (Simonin, 2016). The name "pseudo" means that the models are not related to the kinetics of homogeneous reactions (Bujdák, 2020). The pseudo first order kinetics and its integrated form was postulated by Lagergren in 1898, which took into account the linear driving force of mass transfer at the liquid-solid interface (Shanthi et al., 2014). The PFO mechanism is defined by the Equation 8, if the rate of adsorption is not significant:

$$\frac{dq_t}{dt} = k(q_e - q_t) \qquad \text{Equation 8}$$

where q is adsorption capacity (mg/g); t is time (min) and k is the rate constant. The amount of adsorbed phase (q_t) increases with time (t), attaining a limit at equilibrium q_e, which is the adsorption capacity for this substance after an infinite period of time (Bujdák, 2020; Tan & Hameed, 2017).

The modified pseudo second order kinetic equation (Equation 9), which predicts that the rate of uptake is second order to the available surface sites is defined as:

$$\frac{dq_t}{dt} = k_2(q_e - q_t)^2 \qquad \text{Equation 9}$$

where k_2 is the pseudo-second order (PSO) rate constant. Other symbols are the same as in the PFO model. Like PFO's k, the constant k_2 is a time scale factor that increases with increasing of C_0 (initial concentration of adsorptive (mg/L) in the bulk liquid at time 0). The effect of pH and temperature on k_2 is poorly understood due to the difficulties arising from the influence on the shape of the equilibrium isotherm. A small particle size of adsorbent gives a higher k_2 value due to a lower intraparticle diffusion resistance (Simonin, 2016; Tan & Hameed, 2017).

3.6.1 Adsorption isotherms

An adsorption isotherm depicts the relationship between the equilibrium adsorbate concentrations in the liquid phase and its equilibrium adsorbed amount on the solid phase at a certain temperature (Smernik, 2003). Using these isotherms is possible to model the equilibrium adsorption data for investigation the information about adsorption, for instance: the adsorption mechanisms, the maximum adsorption capacity and the characteristics or properties of solid phases (Wang & Guo, 2020). As can be seen from the Figure 5, the adsorption processes can be described by four general types of isotherms (S, L, H, and C). For the S-type isotherm, the slope first grows with an increase in the adsorption concentration, but eventually goes down and becomes zero as the free areas of the adsorbent are filled. This type of isotherm suggests that the surface has a low affinity for the adsorptive at low concentrations of adsorbate but increases at higher

concentrations. The L-shaped (Langmuir) isotherm is characterized by a decreasing slope as the concentration grows since the free adsorption areas decrease as the adsorbent is filled. This adsorption behavior can be explained by the high affinity of the adsorbent for the adsorptive at low concentrations, which then decreases with increasing concentration. The H-type isotherm, which means high affinity, shows strong adsorbate – adsorptive interactions such as formation of inner-sphere complexes. The C- type isotherm is usually related to adsorption processes of non-polar hydrophobic compounds. The initial slope of this isotherm remains independent of the concentration of the adsorptive until certain maximum adsorption capacity is achieved. The adsorption behavior of this isotherm is characterized by constant partitioning since the partitioning mechanism of organic compound between hydrophobic and hydrophilic phases will indicate C- type isotherm (Essington, 2004; Sposito, 2008).

There are several equilibrium models that can be used for explanation of adsorption processes on the soil surfaces. The most common ones are Freundlich and Langmuir equations. The Freundlich model is empirical model, which describes solute and gas phase adsorption. Meanwhile, Langmuir model connects the coverage of molecules on a solid surface with the concentration of the medium that is above the solid surface at a fixed temperature (Febrianto et al., 2009). The equations of partition coefficient Kp, which can be obtained from the slope of a linear adsorption isotherm and the Freundlich and Langmuir isotherms are mentioned below (Equation 10, Equation 11, Equation 12) :

Partition coefficient:

$$q_e = K_p \times c_e \quad \text{Equation 10}$$

Freundlich equation:

$$q_e = K_F \times c_e^{1/n} \quad \text{Equation 11}$$

Langmuir equation:

$$q_e = c_{max} \times (K_L \times c_e)/(1 + K_L \times c_e) \quad \text{Equation 12}$$

where q_e is the amount of adsorbate per unit mass of adsorbent in (mol kg^{-1}), c_e (mmol L^{-1}) is the equilibrium concentration of the adsorptive; c_{max} (mmol g^{-1}) the maximum sorption capacity of the adsorbent; K_D (L g^{-1}) the distribution coefficient; K_F (L g^{-1}), 1/n (dimensionless) and K_L (L g^{-1}) are constants, K_p partition coefficient (Wang & Guo, 2020).

In general, in modeling of adsorption at equilibrium, Freundlich and Langmuir isotherm are the most widely used. The key difference between them is that the Langmuir curve achieves a plateau figuring out the maximum sorption capacity of the adsorbent for the given adsorbate (Essington, 2004).

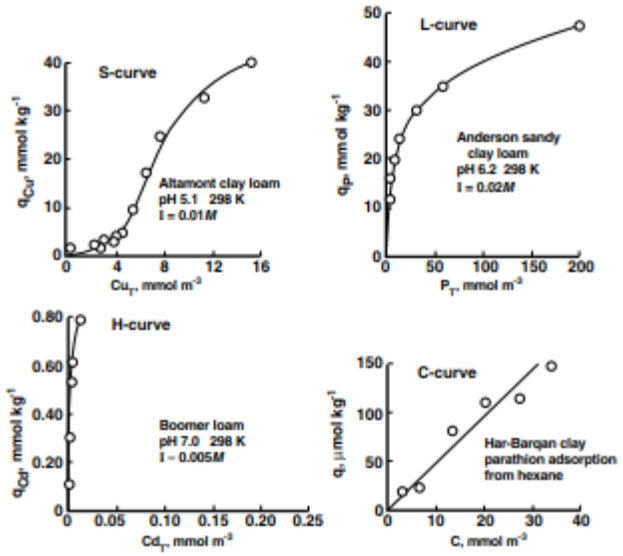

Figure 4 The four general shapes of adsorption isotherms; adapted according to Smernik (2003)

3.6.2 Adsorption edges of metal cations

The adsorption behavior of metals on various adsorbents including minerals can be also described by adsorption edges (Hu et al., 2015). The narrow pH range where metal adsorption increases to almost 100% is traditionally called the adsorption edge (Figure 6). They are also considered as the background for advanced mechanistic adsorption modeling (surface complexation modeling) (Essington, 2004; Smernik, 2003). For comprehending the influence of pH value on the adsorption processes in soils, sediments, SOC (soil organic matter) and other solid materials, the adsorption experiments in a pH gradient are conducted. The position of adsorption edge with respect to pH for a particular metal cation is associated with hydrolysis or acid–base characteristics of this metal.

Besides pH, metal sorption depends on adsorbate/adsorbent concentration, surface coverage and sorbent type (McKenzie, 1980; Smernik, 2003). It is also possible to measure the relative affinity of a cation for the sorbent or the selectivity - a measure of the relative affinity of a particular ion for a given sorbent. The selectivity increases with the decreasing the pH under which cation sorb on a sorbent (Smith, 1999). The selectivity is dependent on the properties of the cation, sorbent, and the solvent.

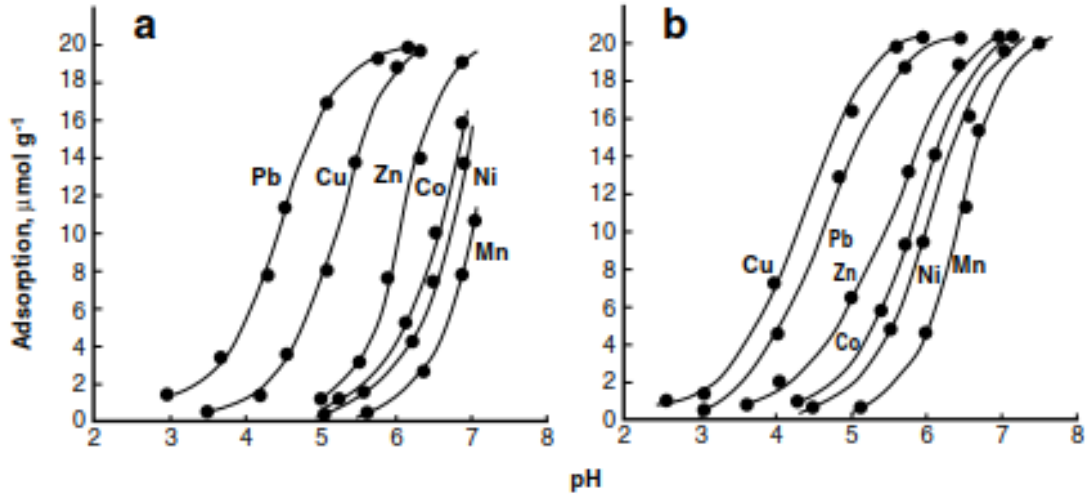

Figure 5 Sorption of Pb, Cu, Zn, Co, Ni, Mn metals on (a) hematite and (b) goethite when they were added at a concentration of 20 µmol/g of adsorbate; adapted according to McKenzie (1980).

$Li^+ < Na^+ < K^+ < Rb^+ < Cs^+$ is the selectivity order of monovalent alkali metal cations, which is associated with the size of hydrated radius. As can be seen from the order above, the element with the smallest hydrated radius is Cs^+; it is able to get as close to the surface as possible and be kept with stiffer bond (Kinniburgh & Jackson, 1981; Smernik, 2003).

The divalent ions are more consistent in selectivity order in comparison with the monovalent ones. The selectivity sequence is also affected by the pH, the type of surface and differences in the H^+/M^{n+} ratios since the ion with the higher H^+/M^{n+} stoichiometry would be preferable at higher pH. The selective adsorption of divalent cations even at low pH values to Fe and Al oxides is also well known. Several spectroscopic studies have demonstrated that divalent metals can form inner sphere complexes and also are more strongly adsorbed in comparison with alkaline earth metals (Smernik 2003; Violante and Pigna 2003; Kinniburgh & Jackson, 1981). According to Jackson (1998), several selective

sequences have been reported for precipitated Fe and Al oxides, Pb > Cu > Zn > Cd > Co > Sr > Mg for Fe-oxide and Cu > Pb > Zn > Cd > Co > Sr > Mg for Al-oxide.

3.7 Metal isotopic fractionation during individual processes

3.7.1 Isotopic fractionation during complexation and sorption

In this chapter, the relationship between extent of metal isotope fractionation and processes such as complexation, adsorption and precipitation will be explained in some extent. The metal isotope fractionation, which can occur due to the thermodynamic differences in bonding environment is likely observed during the formation of aqueous solution complexes or during the binding of metals to the solid surface. The value of coordination number of complexes and bond length (bond "stiffness") can play also significant role in metal isotopic fractionation. For example: the enrichment of about 3‰ in δ^{56}Fe is observed in equilibrium isotope fractionation between aqueous Fe (III) and Fe (II). In this case, enrichment of heavy isotopes tends to be observed in Fe (II), which can be explained by the strong bonding environment or shorter bond length. Additionally, the light Mg isotope enrichment can be observed in organic complexes, which tend to be associated with a longer bong length in comparison with inorganic complexes. For better understanding the effect of complexation to metal isotopes, a lot of experimental data and studies are required. There are some studies regarding the relationship between the complexation of species and equilibrium isotope fractionation, which are available for Cd, Mo, B, Cr, Fe, Ni and etc. (Wiederhold, 2015).

Regarding sorption, most conducted experiments focused on equilibrium isotopic effect (Wiederhold, 2015). Sorption is associated with transportation/transfer of dissolved species from liquid to solid phases such as mineral surfaces. The determination of fraction factor in these studies is important for interpreting the signature of metal isotopes since the fate of metals is often associated with sorption processes. The equilibrium isotope effect during sorption processes mostly occurs due to differences in bonding environment between sorbed and dissolved species. In most cases, the delay for attainment of the equilibrium effect can be faced, because it is difficult to confirm that equilibrium conditions have been achieved. Since usually during sorption processes, the desorption rate is often lower in comparison with adsorption rate. Generally, during sorption processes the isotopic enrichment factor is less than 1‰, but there are exceptions in some

studies (e.g., Mo). For understanding the metal isotopic fractionation during the sorption processes, a lot of studies were conducted with different type of sorbents such as metal oxides (mainly Fe and Mg (oxy-hydro)oxides), clay minerals, bacteria and etc. (Wiederhold, 2015). As an example could be study is Zn isotopic fractionation during adsorption to synthetic birnessite at low (0.01M) and high (0.7M) ionic strength . The results of this research provide the mechanistic explanation for the enrichment of heavier Zn isotopes in natural ferromanganese sediments compared to the deep seawater. The experimental results of this study determined the initial kinetic isotope effect at low ionic strength (lighter isotopes adsorbed, $\Delta^{66/64}Zn_{sorbed\text{-}aqueous} \sim -0.2‰$), which changed over ~ 100 h to almost no isotope fractionation effect (0.05 ± 0.08‰). In comparison with the low ionic strength, the heavy Zn isotopes enrichment that was observed at high ionic strength ($\Delta^{66/64}Zn_{adsorbed\text{-}dissolved}$ up to +2.7‰) reflects the effect of chloro-complexation of Zn in seawater and the equilibrium isotopic fractionation in this study The formation of tetrahedrally coordinated Zn complexes that enriched with the heavier isotopes of Zn most likely occurred due to the low surface loading. But with the increasing of surface load, the proportion of Zn that octahedrally coordinated increased. Therefore, the magnitude of Zn fractionation between adsorbed and dissolved Zn pools decreased from $\Delta^{66/64}Zn_{adsorbed\text{-}dissolved} = 2.74 \pm 0.07‰$ to 0.13 ± 0.07‰ and after was nearly constant at ~ 0.16‰ when the 50% of Zn was adsorbed. That could most likely express the kinetic isotope effect since the lighter isotopes of Zn were adsorbed on mineral surfaces and due to this reason the magnitude of the isotopic fractionation decreased (Bryan et al., 2015). There were some similar observations regarding the increasing proportion of octahedrally coordinated Zn depending on the increasing surface load in other studies (Bryan et al., 2015; Isaure et al., 2005; Little et al., 2014; Toner et al., 2006). Regarding low ionic strength of solution, little or no isotopic fractionation effect was observed between sorbed and dissolved octahedrally coordinated Zn (Bryan et al., 2015).

3.7.2 Cadmium isotopic fractionation during adsorption and precipitation

In this chapter, the relationship of Cd isotopic fractionation with individual processes such as adsorption and precipitation processes will be described in some extent. The knowledge on Cd isotopic fractionation during adsorption to Mn oxyhydroxide

(birnessite) at low (I < 0.01M) and high isotopic strength (I = 0.72M) may be useful and applicable for studying marine biogeochemistry (Wasylenki et al., 2014). Because Cd is the trace micronutrient in the marine environment and plays a proxy role in reconstructing the past global water circulation and water mass mixing (Horner et al., 2010, 2011; Lacan et al., 2006; Wasylenki et al., 2014). The results of the study showed the small fractionation of $\Delta^{114/112}Cd_{\text{fluid–solid}} = +0.12 \pm 0.03‰$ after 24 h at low ionic strength (I < 0.01M) during sorption of Cd to birnessite. It shows that Cd was enriched with lighter isotopes in the sorbed complexes and the heavier isotopes in solution. The reason of this heavier isotope enrichment in fluid could be due to shorter and stiffer bond environment in dissolved Cd in comparison with sorbed complexes. But, in case of high ionic strength (I = 0.72M), the larger fractionation of $^{114/112}Cd_{\text{fluid–solid}} = +0.27 \pm 0.07‰$ was observed, which gradually decreased to 0.12‰ over 912 h. This decrease of the fractionation magnitude could reflect the kinetic isotope effect in the first hours due to sorption of lighter isotopes onto solid phase. But this magnitude was changed over the time due to exchange of sorbed and dissolved species, which could possibly lead to the equilibrium effect. The hypothesis for this high ionic strength behavior is the structural and crystallinity change of birnessite or the change of the sorption mechanism of Cd on solid surface (birnessite).

Another study investigated the isotopic fractionation of cadmium during calcite growth in fresh and sea water (Horner et al., 2011). The experiments in this study Horner et al. (2011) were conducted in artificial seawater and freshwater by controlling the inorganic precipitation of calcite ($CaCO_3$). Before measuring the isotopic composition of Cd, the experiment was conducted under different salinities, temperature, precipitation rate and environment (ambient $[Mg^{+2}]$). Due to the fractionation factor for Cd precipitated into calcite in seawater is always less than one, the preference of lighter Cd isotopes for accumulation in calcite is suggested. The fractionation factor in seawater solution ($\alpha_{CaCO3\text{–}Cd(aq)}$) has the value less than 1 (0.99955 ± 0.00012) in this research, and shows insensitiveness to changes in temperature, precipitation rate and ambient $[Mg^{+2}]$ in this study. Whereas, no isotopic offset was observed in case of $CaCO_3$ growth in freshwater solution ($\alpha_{CaCO3\text{–}Cd(aq)} = 1.0000 \pm 0.0001$) in comparison with the precipitated $CaCO_3$ in artificial seawater. The interpretation of the results indicates the influence of kinetic isotopic effect in this study. The kinetic isotopic fractionation of Cd during the precipitation of calcite or calcite growth can be explained by the largely unidirectional

process, which shows the enrichment of lighter Cd isotopes in the solid phase (calcite) compared to growth solution. Moreover, the different results in experiments with freshwater and seawater indicates the effect of salinity to isotopic fractionation effect. The kinetics of the calcite growth is suggested to be more related to the rate of Cd uptake relative to the total dissolved Cd in solution rather than the exchange between species in solution. In the case of freshwater the uptake of Cd is twice faster than in seawater, which means that kinetic isotopic effect can be modulated via blocking some sites at the crystal surface due to the abundance of some cations (particularly Na^+ and K^+) in higher saline water (seawater). If the concentration of major ions increases (e.g., Na^+ and K^+), the magnitude of ion blocking effect will also increase; however, during the calcite growth uptake rate of Cd will decrease. Consequently, the slower uptake rate of Cd leads to incomplete uptake reaction of which as the result expresses the kinetic isotopic effect (Horner et al., 2011) .

4. Methodology

4.1 Sorbents characterization

Two Fe (oxy)hydroxides, ferrihydrite and goethite, have been used to study the isotopic fractionation of Cd during adsorption onto these two materials. Ferrihydrite (namely a 2-Line Ferrihydrite) was prepared according to the method by Schwertmann and Cornell (2000). Briefly, 40g of $Fe(NO_3)•9H_2O$ was dissolved in 500 mL of deionized water and 330 mL of 1 M KOH were added under vigorous stirring to reach the final pH between 7 and 8. Originated reddish solid precipitates were separated by filtration, washed several times with deionized water and dried at 35°C. Goethite was purchased in a form of Bayoxide® E F 20 (Lanxess). The specific surface area of both oxides was determined using the Brunauer-Emmett-Teller (BET) method and the ASAP 2050 instrument (Micrometrics Instrument Corporation, USA) and amounted to 304.2 m^2/g and 159.4 m^2/g for ferrihydrite and goethite, respectively.

4.2 Adsorption experiments

Adsorption tests evaluating the kinetics of adsorption of Cd onto the ferrihydrite and goethite and the influence of pH on the level of adsorption (adsorption edges) were performed. Firstly, adsorption kinetics was determined. All the adsorption experiments (kinetics and adsorption edges) were performed under the N_2 atmosphere to prevent the precipitation of carbonates. For this purpose, deionized water for test suspensions was firstly over boiled and subsequently cooled down under constant purging with N_2. The test suspensions were prepared with 4 g/L of ferrihydrite or goethite and Cd concentration of 10^{-4} mol/L (Cd isotope standard NIST 3108 Cd). Experiments for both ferrihydrite and goethite variants were performed under 3 different ionic strengths: 0.1, 0.01 and 0.001 mol/L $NaNO_3$ and pH 7 (controlled by the $NaOH/HNO_3$). The suspensions saturated with N_2 were then agitated for different times up to ~200 hours – a separate batch was used for each time interval. After each time period, samples were immediately filtered through a 0.2 µm nylon syringe filter and concentration of Cd in filtrate was determined using inductively coupled plasma optical emission spectrometry (ICP OES; 720 Series, Agilent Technologies). The amount of Cd adsorbed to the ferrihydrite/goethite was calculated as

the difference between the original concentration of Cd in solution and concentration after adsorption. The obtained kinetic data were subsequently modeled using pseudo-second-order equation, which is a common model used for similar adsorption studies (Kalantari et al. 2015; Karami 2013).

In case of experiments focused on adsorption edges, test suspensions were prepared similarly as in case of kinetic experiments, i.e., 4 g/L of ferrihydrite/goethite, ionic strengths of 0.1, 0.01 and 0.001 mol/L $NaNO_3$ and Cd concentration of 10^{-4} mol/L (Cd isotope standard NIST 3108 Cd). In case of batches for adsorption edges determination, oxide powders were added to the metal solutions and the pH was adjusted (under constant purging with N_2) using $NaOH/HNO_3$ to be within the range from ~2.5 to ~10. Batches with adjusted solutions saturated with N_2 were closed tightly let to equilibrate for 24 hours under constant agitation. After 24 hours, batches were opened, and the pH was measured again using the pH meter under constant purging with N_2. Immediately after that, samples were centrifuged (15 mins, 7000 rpm), filtered through a 0.2 µm nylon syringe filter and concentration of Cd in filtrate was determined using ICP-OES. The amount of Cd adsorbed to the solid phase was calculated in the same way as in case of kinetic experiments.

4.3 Isotopic analyses

After the ICP-OES analysis, chosen filtrates from the adsorption edges experiments have been analyzed for the isotopic fractionation of Cd. Prior to the direct measurements, samples were separated on the chromatographic columns following the methods by Schmitt et al. (2009a, 2009b) and Abouchami et al. (2011, 2014). The protocol for Cd separation (Table 4) was adapted in our laboratory using 400 µL of BioRad AG1-X8 anion exchange resin (100-200 mesh) in bromide form. Before separation itself, liquid samples were evaporated and converted to the bromide form.

Table 4 Protocol for Cd separation and preparation of filaments for thermal ionization mass spectrometry (TIMS)

2 ml Column BioRad + 0.4 ml Resin AG1-X8 100-200 mesh							
Order	**Process**	**Step**	**Reagent**	**Volum**	**Number of doses**	**Dose**	**Note**
Part I	*Washing column*	1	HNO_3 (0.5M) **normal pur**	4 ml	2	2 ml	
		2	H_2O MQ	4 ml	2	2 ml	
Part II	*Conditionning*	1	HNO_3 (0.5M)-HBr (0.2M) ultrapur	4 ml	4	1 mL	
Part III	*Sample Loading*	1	HNO_3 (0.5M)-HBr (0.2M) ultrapur	2 ml	4	0.5 ml	*Has to be totally dissolved*
Part IV	*Matrix elution*	1	HNO_3 (0.5M)-HBr (0.2M) ultrapur	2 ml	4	0.5 mL	
		2	HNO3 (0.45M)-HBr (0.03M) ultrapur	3 ml	3	1 ml	
Part V	*HBr Removing*	1	HNO_3 (0.25M) ultrapur	100 µl	1	100 µl	
Part VI	*Cd recovery*	1	HNO_3 (0.25M) ultrapur	6 ml	6	1 mL	
Part VII	*Evaporation* ***until last drop***	1					
Part VIII	*Conditionning for filament*	1	H_3PO_4 cleaned	50 µl	1	50 µl	**for 500 ng of Cd**
		2	Si gel cleaned	100 µl	1	100 µl	
Part IX	*Evaporation*	1	remove from the hot plate before burning				**no more than 110 °C**

Part X	*Dissolution*	1	HNO_3 (2%) ultra pur	10-15 µl	1	10-15 µl	Use ultrasound bath

Recovered Cd solutions after column separation were evaporated on a hot plate until the last drop (110 °C-120 °C) and after cooling down, an activator consisting of 50 µL of H_3PO_4 0.1 N and 100 µL of silica gel (100 mg/L of Si) per 500 ng of Cd was added to the sample. The sample was subsequently evaporated until the dryness, taken in 15 µL of HNO_3 2% and stepwise loaded onto outgassed single Re filaments. Cadmium isotope ratios were measured by thermal ionization mass spectrometry using a Triton (Thermo Fisher) instrument.

The Cd isotopic compositions were reported as $\delta^{114/110}$Cd, relative to the NIST SRM 3108 (Equation 13):

$$\delta^{114/110}Cd = \left(\frac{\left(\frac{^{114}Cd}{^{110}Cd}\right)_{sample}}{\left(\frac{^{114}Cd}{^{110}Cd}\right)_{NIST\ SRM\ 3108}} - 1 \right) \times 1{,}000 \qquad \text{Equation 13}$$

The measurements were corrected with respect to potential Cd isotope fractionation during column separation and measurement using double-spiking method. The double-spike reduction was based on nested iteration method (algorithm designed by Dr. Thomas Bullen). The double spike was prepared by mixing two enriched Cd isotopic spikes: ^{106}Cd (97 %) and ^{116}Cd (99 %) (IsoFlex, USA). The $\delta^{114/110}$Cd value measured for the NIST SRM 3108 was ± 0.02 ‰ (2SD, n=3).

5. Results

5.1 Adsorption edges of Cd on goethite

The Figure 6 depicts the adsorption edges of Cd on goethite at different ionic strengths (0.001M, 0.01M and 0.1M $NaNO_3$), demonstrating the relationship between the adsorbed Cd amount (%) and pH value. The adsorbed amount of Cd on goethite starts increasing from the zero at pH value of 5 at ionic strength of 0.001M, 0.01M and 0.1M $NaNO_3$. The amount of adsorbed of Cd on goethite at the ionic strengths of 0.001M, 0.01M and 0.1M $NaNO_3$ experienced the increase with the shifting of adsorption edge to the higher region pH. It means that the adsorption process in case of Cd is highly pH dependent. The significant amount of Cd was adsorbed on goethite between pH 6 – 8, where the maximum amount of adsorbed Cd was reached approximately at pH 8. The adsorption edges indicate the low affinity of Cd to goethite at the lower pH values. There are some negative adsorption values in case of high ionic strength of solution (0.1 M $NaNO_3$), this error could be occurred due to the experimental/measurement uncertainties.

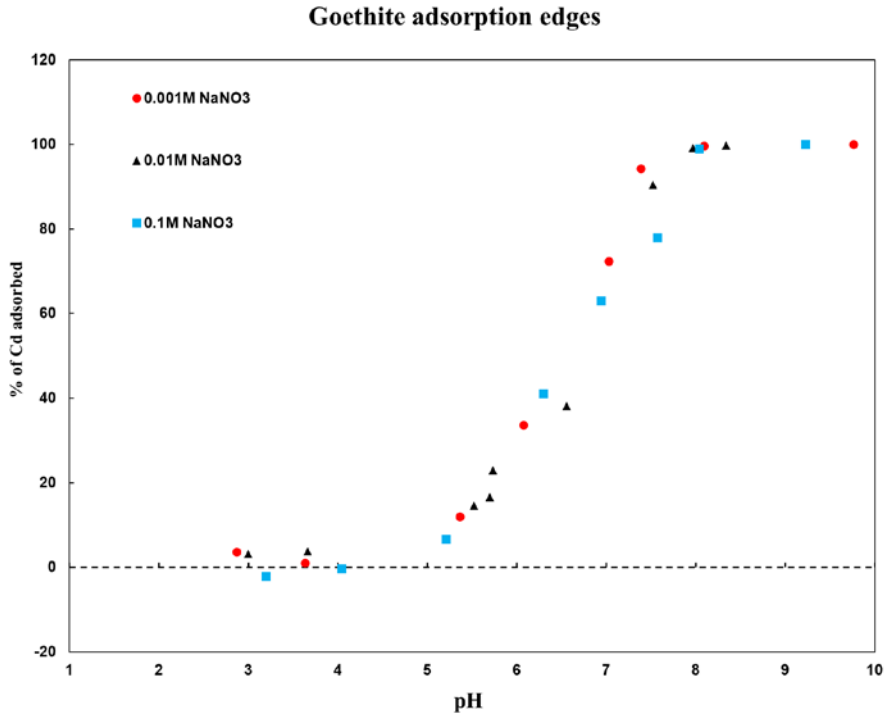

Figure 6 The adsorption edges of Cd on goethite at different ionic strengths (0.001M, 0.01M and 0.1M $NaNO_3$).

5.2 Adsorption edges of Cd on ferrihydrite

As can be seen from Figure 7, the adsorption edges of Cd on ferrihydrite at various ionic strengths (0.001M, 0.01M and 0.1M $NaNO_3$) depict the relationship between the adsorbed Cd amount (%) and pH value. The amount of adsorbed Cd on ferrihydrite at the ionic strengths of 0.001M, 0.01M and 0.1M $NaNO_3$ grew with the increasing pH value. As mentioned in chapter 4.1, the adsorption process is highly pH dependent. The adsorbed amount of Cd on goethite starts increasing from the zero at pH value of 5.5 at ionic strength of 0.001M, 0.01M and 0.1M $NaNO_3$. But the high amount of Cd was adsorbed on ferrihydrite between at pH 6 – 7, where the maximum amount of adsorbed Cd was reached at pH 7.5. The adsorption edges indicate the low affinity of Cd to ferrihydrite at the lower pH values. It is also noticeable that the ionic strength of solution does not significantly impact the adsorption of Cd on goethite and ferrihydrite. There are some negative adsorption values in case of various ionic strength of solution (0.001M, 0.01M, 0.1M $NaNO_3$), this inconsistency could be associated with the experimental/measurement inaccuracies.

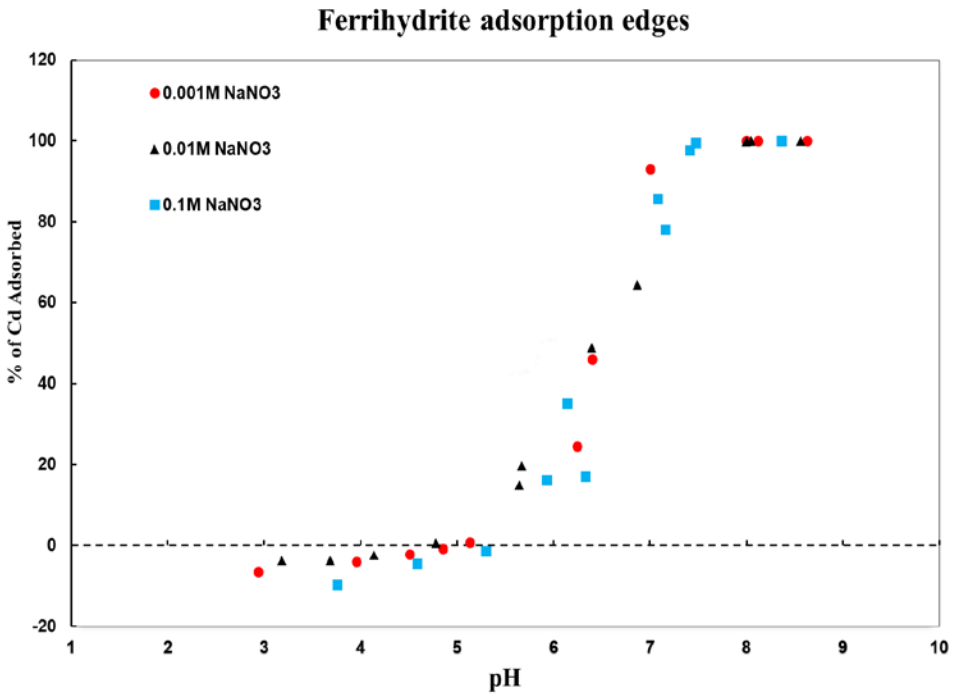

Figure 7 The adsorption edges of Cd on ferrihydrite at different ionic strengths (0.001M, 0.01M and 0.1M $NaNO_3$).

5.3 Adsorption kinetics of Cd – Goethite

As can be seen from Figure 8, the kinetic curves of Cd on goethite at various ionic strengths (0.001M, 0.01M and 0.1M $NaNO_3$) demonstrate the relationship between the adsorbed Cd amount (%) and time. To assess the kinetic rate of adsorbed Cd on goethite, the kinetic parameters of pseudo second model are depicted in Table 5. The adsorption kinetic data from Figure 8 shows that the high amount Cd was rapidly adsorbed by goethite in first 15 minutes and achieved equilibrium within/after (~80 <) hours at various ionic strengths of solution (0.001M, 0.01M, 0.1M $NaNO_3$). It is visible that highest amount of adsorbed Cd was recorded at the lowest ionic strength of solution. This is an indication of ionic strength effect on adsorption processes. A reasonable explanation for this could be the lower competition between Cd^{+2} and Na^{+} for available sites on mineral surface since at the lowest ionic strength is the less amount of Na^{+} ions. Another important point is that the k_2 values in case of goethite are higher in comparison with ferrihydrite, which means that the adsorption rate of goethite is also higher than that of ferrihydrite (Table 5,Table 6). Meanwhile, the amount of adsorbed Cd on goethite (Figure 8) under given conditions (pH 7) is less than that of ferrihydrite (Figure 9).

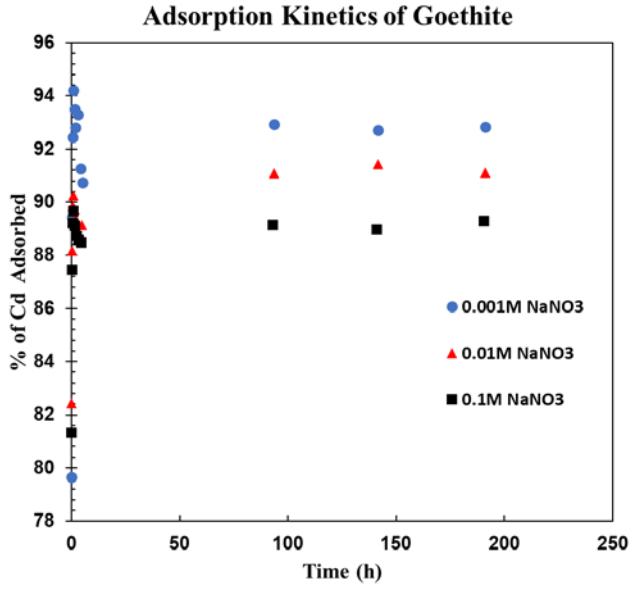

Figure 8 The amount (%) of Cd adsorbed on ferrihydrite versus time at various ionic strength (0.001M, 0.01M, 0.1M $NaNO_3$).

Table 5 Kinetic parameters for Cd adsorption on ferrihydrite at various ionic strength (0.001M, 0.01M, 0.1M $NaNO_3$).

Pseudo-second order				
Goethite				
	Ionic strength	k2 (g/mg/min)	qe (mg/g)	R2
Cd(II)	0.001M	0.3886	2.6865	1
	0.01M	0.2034	2.6982	1
	0.1M	0.3081	2.4708	1

5.4 Adsorption kinetics of Cd – Ferrihydrite

The provided kinetic curves for Cd adsorption on ferrihydrite at various ionic strengths (0.001M, 0.01M, 0.1M $NaNO_3$) (Figure 9) illustrate the relationship between the adsorbed amount of Cd (%) and time. The constants calculated for the pseudo second order kinetic model are provided in Table 6 for evaluating the kinetic rate of adsorbed Cd on ferrihydrite. As can be seen from Figure 9, the high amount of Cd was rapidly adsorbed by ferrihydrite in 15minutes and achieved equilibrium within/after (~30 <) hours at various ionic strength of solution (0.001M, 0.01M, 0.1M $NaNO_3$). It is visible that there is not a significant effect of ionic strength to the adsorbed amount of Cd on ferrihydrite. But it would be also important to point out that the differences between the k_2 values at all ionic strengths (0.001M, 0.01M, 0.1M $NaNO_3$) do not significantly vary, which indicates non-significant impact of ionic strength on the rate of adsorption.

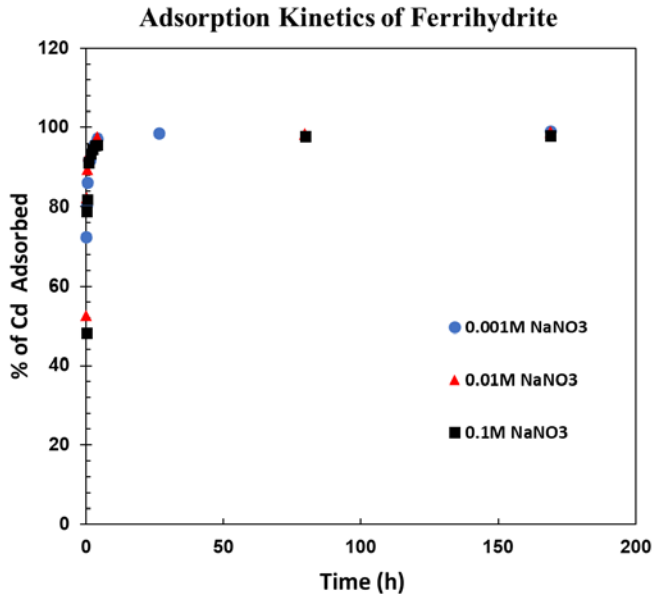

Figure 9 The amount (%) of Cd adsorbed on ferrihydrite versus time at various ionic strength (0.001M, 0.01M, 0.1M $NaNO_3$).

Table 6 Kinetic parameters for Cd adsorption on ferrihydrite at various ionic strength (0.001M, 0.01M, 0.1M $NaNO_3$).

Pseudo-second order				
Ferryhydrite				
	Ionic strength	k2 (g/mg/min)	qe (mg/g)	R2
Cd(II)	0.001M	0.0675	2.8542	1
	0.01M	0.0604	2.9250	1
	0.1M	0.0649	2.7567	1

5.5 Isotopic fractionation of Cd in aqueous solution during adsorption on goethite and ferrihydrite

Adsorption experiments were coupled with isotopic analyses to determine the isotopic fractionation between sorbed and dissolved Cd in relation to varying proportion of Cd adsorbed to goethite and ferrihydrite. Unfortunately, within the timeframe of the thesis, only the $\delta^{114/110}$ Cd values for the isotopic fractionation of Cd in aqueous phase were measured. The analyses aiming at the $\delta^{114/110}$ Cd in solid phase have delayed due to COVID-19 situation and are planned in close future.

As can be seen from Figure 10, calculated average equilibrium isotopic fractionation of Cd in aqueous solution during adsorption on goethite was $\Delta^{114/110}Cd_{aqueous\text{-}sorbed}$ = +0.18‰ and on ferrihydrite $\Delta^{114/110}Cd_{aqueous\text{-}sorbed}$ = +0.48‰. To compare the potential influence of kinetics, the Rayleigh fractionation model based on the same parameters was depicted too. The $\delta^{114/110}$ Cd values in aqueous solution during adsorption on goethite are staying positive irrespective the ionic strength of solution, indicating the Cd heavier isotope enrichment in aqueous phase. The same is noticeable in the case of ferrihydrite, here we also can notice the heavier isotopic enrichment of Cd in solution. The more Cd is adsorbed from liquid phase, the heavier composition of aqueous phase will be (Wasylenki et al., 2014).

As can be seen from the data below, the average fractionation in aqueous solution for ferrihydrite is higher than for goethite. It can be interpreted as the higher enrichment of heavy isotopes in aqueous solution of ferrihydrite in comparison with goethite. Regarding the isotopic fractionation of Cd on goethite and ferrihydrite mineral surfaces, unfortunately, were not able to measure the data directly, which could further confirm the

influence of equilibrium isotopic effect or enable more precise calculation of $\Delta^{114/110}Cd_{aqueous\text{-}sorbed}$. Yet, even from the fractionation data provided for aqueous phase in Figure 10, better correlation with linear trend is visible, suggesting the predominant influence of equilibrium isotopic fractionation effect rather than the kinetic isotopic effect, depicted using Rayleigh model.

At the end, I would like to mention that there is no a significant effect of ionic strength to the isotopic fractionation of Cd during adsorption on ferrihydrite and goethite, which is visible from Figure 10.

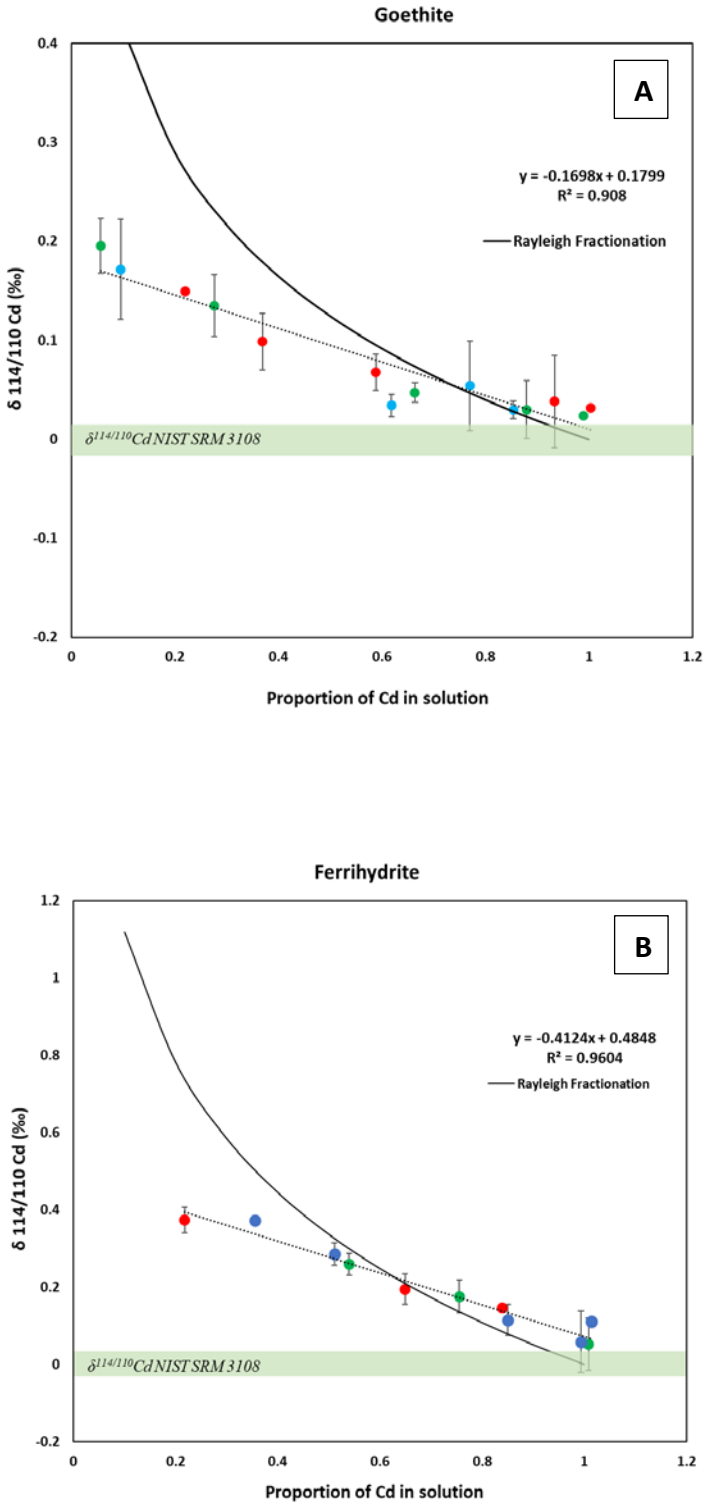

Figure 10 Isotopic composition of Cd in aqueous solution during sorption on goethite (A) and ferrihydrite (B) at ionic strength of 0.001M (green circle), 0.01M (blue circle), 0.1M $NaNO_3$ (red circle) versus proportion of Cd in solution. Vertical error bars show the standard deviation (2sd) on 2-3 replicate analyses of each sample. The dashed lines indicate the linear trends of equilibrium fractionation with $\Delta^{114/110}Cd_{aqueous\text{-}sorbed}$ = +0.18‰ for goethite and $\Delta^{114/110}Cd_{aqueous\text{-}sorbed}$ = +0.48‰ for ferrihydrite, and the solid lines are Rayleigh fractionation curves.

6. Discussion

6.1 pH and ionic strength effect.

As we mentioned in chapter 4.1, the adsorption of cadmium on goethite and ferrihydrite is pH dependent. The low affinity of Cd to goethite and ferrihydrite at lower pH could be due to the positively charged surface of minerals (Figure 6, Figure 7). The surface is charged positively because pH is below the pH_{PZC} (Point of Zero Charge) of goethite and ferrihydrite. In Krumina et al. (2016) study about desorption mechanisms of phosphate from ferrihydrite and goethite surfaces the reported PZC values are 8.1 and 9.5 respectively. The positively charged surface can repel metal cations at lower pH (acidic conditions). But with the shifting adsorption edge of pH to higher region, the repulsion interaction between Cd (II) and H^+ was weaker and the surface started being charged more with negatively charged functional groups (Ogata et al., 2020). Due to this shifting of pH, the fast adsorption was observed in case of goethite and ferrihydrite at pH ~ 5 - 8.5. This also gives opportunity to metals ions to form inner-sphere complexes by chemisorption on the surface of mineral phases (Strawn & Bohn, 2015). Regarding the ionic strength of solution, we didn't observe a significant influence on the adsorption of Cd on goethite and ferrihydrite in our results.

The adsorption kinetics and PSO (pseudo second order) parameters proves the extent of influence of ionic strength on adsorption rate of Cd on goethite and ferrihydrite. The maximum amount of adsorbed Cd on goethite in mentioned time range in result section is highest at weakest ionic strength of solution; however, in case of ferrihydrite there is no a significant effect of ionic strength on the adsorbed amount of Cd. As we discussed previously in chapter 4.3, it can be associated with the less competition of Cd^{+2} and Na^+ ions for free sites on the surface of goethite. Moreover, the adsorbed amount of Cd on goethite was less in comparison with ferrihydrite. But the adsorption rate of goethite is higher than that of ferrihydrite, as can be seen from the calculated k_2 (Table 5, Table 6). As one of the reasonable explanations of this can be the differences of sorption capacities and surface areas between these two mineral phases, where the ferrihydrite (304 m^2/g) has the larger surface area than goethite (159 m^2/g). The size of pores are major contributors to the adsorption ability and play a significant role in adsorption processes of adsorbates to adsorbent (Ogata et al., 2020). The interpretation of the result

in terms of importance of pore sizes and sorption capacity was achieved in study of selective sorption of cadmium by mixed oxides of iron and silicon, where the sorption capacity of mixed oxides is greater than SiO_2 and $Fe(OH)_3$ (Mustafa et al., 2010). The importance of surface area of ferrihydrite and goethite also mentioned in study of Julliot et al. (2008), where ferrihydrite adsorbed more Zn in comparison to goethite.

6.2 Causes of isotopic fractionation at low and high ionic strength

As mentioned in previous result section, due to the situation with COVID-19 pandemic we were not able to obtain the results of isotopic fractionation of Cd in solid phase within the timeframe of the thesis; however, these experiments are planned in close future.

Firstly, it is needed to mention that we have not noticed any significant effect of the ionic strength of solution to isotopic fractionation of Cd. The average magnitude of isotopic fractionation of Cd in aqueous solution during sorption on goethite is $\Delta^{114/110}Cd_{aqueous\text{-}sorbed}$ = +0.18‰ and ferrihydrite is $\Delta^{114/110}Cd_{aqueous\text{-}sorbed}$ = +0.48‰. The isotopic fractionation of Cd also increases with the decreasing of the proportion of Cd in aqueous solution and increasing its loading on mineral surfaces. Both results are indication of stable enrichment with heavier isotopes of Cd in aqueous solution. Since we did not provide isotopic fractionation of Cd in solid phases (goethite and ferrihydrite) it is not possible to unambiguously identify the type of metal isotopic effect in our study yet the linear trend observed for the data in Figure 9 and 10 suggests probable major contribution of equilibrium isotopic effect. According to our data, we hypothesize that different magnitude of isotopic fractionation of Cd in aqueous solution of goethite and ferrihydrite under certain conditions could be due to the differences in bonding strength and the different complexation mechanism that can be driven by the coordination chemistry of metal species. Additionally, the heavier isotopic enrichment in aqueous solution can be explained by the lower coordination number of metal species, and stiffness/shortness of bonds between species in fluid phase. Our hypothesis could be confirmed by EXAFS (Extended X-ray absorption fine structure) that can determine the coordination chemistry of metal species and bond length between species. There are some studies which reported the atomic radius of Cd-O in aqueous solution and adsorbed Cd on solid phases. We expect that the lengths of Cd-O bond in aqueous solution is slightly

shorter in comparison with the adsorbed Cd to goethite and ferrihydrite and due to this reason, we observed the heavier isotopic enrichment in aqueous solutions.

There is a study about the structures of cadmium iodide complexes in water and DMSO (Dimethyl sulfoxide) solutions, where Ohtaki (1981) determined a Cd-O bond length of 2.29 Å by X-ray diffraction in perchlorate solution. The almost same value for the length of Cd-O bond (2.27 ± 0.01 Å) was observed in the study of Cd adsorbed to kaolinite, but in this case, no differences between the Cd-O distances of Cd adsorbed to kaolinite and aqueous Cd (2.27 Å) in solution were observed . It was suggested to correspond with the outer-sphere complexation, where the authors concluded from Cd–Si distances that a significant proportion of sorbed Cd was in outer-sphere complexes at the mineral surface for maintaining its hydration shell (Vasconcelos et al., 2008). The Cd-O bond length of 2.29 Å is also in a good agreement with EXAFS results of Lorenzo (1994) and (Boily et al., 2005). But in Lorenzo (1994) study about structure and stability of Cd^{+2} surface complexes on ferric oxides is mentioned that the Cd-O bond length is reduced when Cd ions replace Fe ions in goethite.

Although not the case of Cd, Julliot et al. (2008) performed similar study demonstrating the difference between the length and strength of Zn-O bonds in mineral phases (goethite and ferrihydrite) and aqueous solution. Additionally, it also explains the relationship between the bonding environment and isotopic behavior of Zn during sorption on goethite and ferrihydrite. The average isotopic fractionation for ferrihydrite is $\Delta^{66/65}Zn_{aqueous\text{-}sorbed}$ = +0.53‰ and for goethite is $\Delta^{66/65}Zn_{aqueous\text{-}sorbed}$ = +0.29‰, giving similar fractionation magnitudes as in case of our study, with the difference of enrichment of heavier Zn isotopes in solid phase. This difference in isotopic fractionation can be related to stronger Zn-O bonding environment in the Zn-ferrihydrite surface complex in comparison to the Zn-goethite one. According to the EXAFS result, the average length of Zn-O bond for adsorbed Zn on ferrihydrite is 1.96 Å. The bond valence of Zn-O bonds in the tetrahedrally coordinated Zn complexes is 0.51 (v.u.). In case of goethite the length of the Zn-O bond in the octahedrally coordinated Zn is 2.06 Å and the average bond strength is equal to 0.39 (v.u.). For explanation the difference of isotopic fractionation behavior of adsorbed Zn on mineral surfaces, the length and strength values of the Zn-O bonds in sixfold coordinated Zn complex of aqueous solution should be also mentioned. The bond valence of sixfold coordinated Zn in water is 0.32 (v.u.) and the length of Zn-O bonds is 2.11 Å. From these demonstrated values we can see that differences in bond

strength between Zn/goethite and aqueous Zn is quite low (0.07 v.u.), this could be a reason of the low isotopic fractionation $\Delta^{66/65}Zn_{aqueous\text{-}sorbed}$ = +0.29‰. This low value also could indicate that no changes in coordination chemistry was occurred between sorbed and aqueous Zn. But in case of ferrihydrite we can observe the large difference in the bond strength (0.19 v.u.) which is an indication of the larger isotopic fractionation ($\Delta^{66/65}Zn_{aqueous\text{-}sorbed}$ = +0.53‰). In overall, the results also indicate the enrichment of heavier Zn isotopes on goethite and ferrihydrite compared to dissolved Zn in solution. Our hypothesis can be in a good agreement with this study since the heavier isotopic enrichment is associated with stiffer bonding environment. Moreover, the difference in isotopic fractionation of Cd in ferrihydrite ($\Delta^{114/110}Cd_{aqueous\text{-}sorbed}$ = +0.48‰) and goethite ($\Delta^{114/110}Cd_{aqueous\text{-}sorbed}$ = +0.18‰) can also be related to the difference of Cd-O bond strengths between these mineral phases and aqueous Cd.

7. Conclusion

We conducted several experiments demonstrating the influence of pH to adsorption of Cd to goethite and ferrihydrite at different ionic strength of solution (0.001M, 0.01M, 0.1M $NaNO_3$). The adsorption kinetic experiments at the same ionic strengths were also conducted for the determination of the relationship between the adsorbed amount of Cd (%) and time. PSO (pseudo second order) equation was applied for distinguishing the rate of adsorbed Cd on goethite and ferrihydrite. As an addition to this we provided the results of experiments that was conducted for Cd isotopic fractionation during adsorption on ferrihydrite and goethite at ionic strength of 0.001M, 0.01M, 0.1M $NaNO_3$. The main findings of our study are summarized below:

1. The amount of adsorbed Cd on goethite and ferrihydrite increases with the shifting of adsorption edge to the higher region of pH. The low affinity of Cd to goethite and ferrihydrite was observed at lower pH.

2. The maximum amount of adsorbed Cd on goethite was recorded at the lowest ionic strength of solution, which could be associated with less competition between Cd^{+2} and Na^{+} ions for available sites on goethite, meanwhile no significant influence of the ionic strength of solution was observed in case of adsorbed Cd on ferrihydrite. The amount of adsorbed Cd (%) on goethite over the time is less than that of ferrihydrite because of higher specific surface of ferrihydrite in comparison with goethite. The calculated value of k_2 for adsorption of Cd to goethite is higher than that of ferrihydrite, which indicates that the adsorption rate of Cd on ferrihydrite is lower than in case of goethite.

3. The calculated average equilibrium isotopic fractionation magnitudes of Cd in aqueous solution during sorption on ferrihydrite and goethite are $\Delta^{114/110}Cd_{aqueous\text{-}sorbed}$= +0.48‰ and $\Delta^{114/110}Cd_{aqueous\text{-}sorbed}$ = +0.18 ‰ respectively. The positive value of isotopic fractionation in aqueous solution indicates the heavier isotopic enrichment of Cd in solution. We hypothesize that the recorded difference between isotopic fractionation of Cd in aqueous solution during sorption on ferrihydrite and goethite is associated with the stiffness/ length and strength of Cd-O bonds. We expect that the Cd-O bonds are stiffer in aqueous solution than on the surface of ferrihydrite and goethite. The difference in the bond valence of Cd-O in ferrihydrite and aqueous solution could be larger than those of

goethite and aqueous solution, which then could be a reason for observed higher isotopic fractionation of Cd in aqueous solution of ferrihydrite. Additionally, the observed isotopic fraction was attributed mostly to the equilibrium isotopic effect since the experimental data were fitting rather the isotopic equilibrium trend line than the Rayleigh model.

In conclusion, I would like to point out that these results indicate the strong need for study continuation to elucidate more the underlaying mechanisms. The EXAFS analysis aiming at the Cd adsorbed to goethite and ferrihydrite have been already performed and the data are currently under treatment. Also, the $\delta^{114/110}$ Cd values are going to be measured soon. Coupling the direct EXAFS measurements together with the complete Cd isotopic fractionation data will thus provide a background for better understanding the mechanisms controlling the complexation and isotopic fractionation of Cd with two important environmental sorbents, ferrihydrite and goethite.

8. References

Abouchami, W., Galer, S. J. G., De Baar, H. J. W., Alderkamp, A. C., Middag, R., Laan, P., ... & Andreae, M. O. (2011). Modulation of the Southern Ocean cadmium isotope signature by ocean circulation and primary productivity. *Earth and Planetary Science Letters*, *305*(1-2), 83-91.

Abouchami, W., Galer, S. J. G., De Baar, H. J. W., Middag, R., Vance, D., Zhao, Y., ... & Andreae, M. O. (2014). Biogeochemical cycling of cadmium isotopes in the Southern Ocean along the Zero Meridian. *Geochimica et Cosmochimica Acta*, *127*, 348-367.

Adriano, D. C. (2001). *Trace Elements in Terrestrial Environments* (Second Edition). Springer-Verlag New York Berlin Heidelberg. https://doi.org/https://doi.org/10.1007/978-0-387-21510-5

Amanullah, M., Viswanathan, S., & Farooq, S. (2000). Equilibrium, kinetics, and column dynamics of methyl ethyl ketone biodegradation. *Industrial and Engineering Chemistry Research*, *39*(9), 3387–3396. https://doi.org/10.1021/ie000265m

Baskaran, M. (2012). *Handbook of environmental isotope geochemistry* (Vols. 1–2, Issue June). Springer-Verlag Berlin Heidelberg. https://doi.org/10.1007/978-3-642-10637-8

Berna, E. C. (2010). Cr stable isotopes as indicators of Cr (VI) reduction in groundwater: A detailed time-series study of a point-source plume. *Environmental Science and Technology*, 44(3), 1043-1048. Retrieved from https://doi.org/10.1021/es902280s

Boily, J. F., Jöberg, S., & Persson, P. (2005). Structures and stabilities of Cd (II) and Cd (II) phthalate complexes at the goethite/water interface. *Geochimica et Cosmochimica Acta*, *69*(13), 3219–3235. https://doi.org/10.1016/j.gca.2004.12.013

Bryan, A. L., Dong, S., Wilkes, E. B., & Wasylenki, L. E. (2015). Zinc isotope fractionation during adsorption onto Mn oxyhydroxide at low and high ionic strength. *Geochimica et Cosmochimica Acta*, *157*, 182–197. https://doi.org/10.1016/j.gca.2015.01.026

Bujdák, J. (2020). Adsorption kinetics models in clay systems. The critical analysis of pseudo- second order mechanism. *Applied Clay Science*, *191*(February), 1–7. https://doi.org/10.1016/j.clay.2020.105630

Chopping, G. R., Lijenzin, J. O., & Rydberg, J. (2002). Unstable Nuclei and Radioactive Decay. In *Radiochemistry and Nuclear Chemistry* (Third Edit, pp. 58–93). Butterworth-Heinemann. https://doi.org/10.1016/b978-075067463-8/50004-2

Chuanwei, Z. (2015). Isotopic Geochemistry of Cadmium: A review. In *Acta Geologica Sinica* (pp. 2048–2057). Geological Society of China.

Essington. (2004). *Soil and Water Chemistry: An Integrative Approach* (pp. 334–358). CRC Press. Boca Ranton.

Febrianto, J., Natasia, A., Sunarso, J., Ju, Y., Indraswati, N., & Ismadji, S. (2009). Equilibrium and kinetic studies in adsorption of heavy metals using biosorbent: A summary of recent studies. *Journal of Hazardous Materials*, *162*, 616–645. https://doi.org/10.1016/j.jhazmat.2008.06.042

Hoefs, J. (1997). *Stable Isotope Geochemistry*. New York: Springer-Verlag.

Horner, T. J., Rickaby, R. E., & Henderson, G. M. (2011). Isotopic fractionation of cadmium into calcite. *Earth and Planetary Science Letters*, *312*(1–2), 243–253. https://doi.org/10.1016/j.epsl.2011.10.00

Horner, T. J., Schönbächler, M., Rehkämper, M., Nielsen, S. G., Williams, H., Halliday, A. N., Xue, Z., & Hein, J. R. (2010). Ferromanganese crusts as archives of deep water Cd isotope compositions. *American Geophysical Union*, *11*(4), 1–10. https://doi.org/10.1029/2009GC002987

Huang, C. P., & Stumm, W. (1973). Specific adsorption of cations on hydrous γ-Al_2O_3. *Journal of Colloid and Interface Science*, 43, 409–420.

Hu, Q., Xiao, Z., Xiong, X., Zhou, G., & Guan, X. (2015). Predicting heavy metals' adsorption edges and adsorption isotherms on MnO2 with the parameters determined from Langmuir kinetics. *Journal of Environmental Sciences (China)*, *27*(C), 207–216. https://doi.org/10.1016/j.jes.2014.05.036

Isaure, M. P., Manceu, A., & Nicolas, G. (2005). Zinc mobility and speciation in soil covered by contaminated dredged sediment using micrometer-scale and bulk-averaging X-ray fluorescence. *Geochimica et Cosmochimica Acta*, *69*(5), 1173–1198. https://doi.org/10.1016/j.gca.2004.08.024

Jackson, T. A. (1998). The Biogeochemical and Ecological Significance of Interactions between Colloidal Minerals and Trace Elements. In *Environmental Interactions of Clays* (pp. 93–205). Springer-Verlag Berlin Heidelberg. https://doi.org/10.1007/978-3-662-03651-8_5

Julliot, F., Marechal, C., Cacaly, S., Morin, G., Ponthieu, M., & Mare, C. (2008). Zn isotopic fractionation caused by sorption on goethite and 2-Lines ferrihydrite. *Geochimica et Cosmochimica Acta*, *72*, 4886–4900. https://doi.org/10.1016/j.gca.2008.07.007

Kabata-Pendias, A., & Pendias, H. (2001). Biogeochemistry of trace elements. In *Trace Elements in Soils and Plants, Third Edition* (Vol. 2nd, Issue 2, p. 881). https://doi.org/10.1201/b10158-25

Kalantari, K., Ahmad, M. B., Masoumi, H. R. F., Shameli, K., Basri, M., & Khandanlou, R. (2015). Rapid and high capacity adsorption of heavy metals by Fe3O4/montmorillonite nanocomposite using response surface methodology: Preparation, characterization, optimization, equilibrium isotherms, and adsorption kinetics study. *Journal of the Taiwan institute of Chemical Engineers*, *49*, 192-198

Karami, H. (2013). Heavy metal removal from water by magnetite nanorods. *Chemical Engineering Journal*, *219*, 209-216.

Kinniburgh, D. G., & Jackson, M. L. (1981). Cation adsorption by hydrous metal oxides and clay. In E. M. A. Anderson and A. J. Rubin, *Adsorption of Inorganics at Solid–Liquid Interfaces* (pp. 91-160). Ann Arbor Sci., Ann Arbor, MI.

Krumina, L., Kenney, J. P. L., Loring, J. S., & Persson, P. (2016). Desorption mechanisms of phosphate from ferrihydrite and goethite surfaces. *Chemical Geology*, *427*, 54–64. https://doi.org/10.1016/j.chemgeo.2016.02.016

Lacan, F., Francois, R., Ji, Y., & Sherrell, R. M. (2006). Cadmium isotopic composition in the ocean. *Geochimica et Cosmochimica Acta*, *70*(20), 5104–5118. https://doi.org/10.1016/j.gca.2006.07.036

Little, S. H., Sherman, D. M., Vance, D., & Hein, J. R. (2014). Molecular controls on Cu and Zn isotopic fractionation in Fe – Mn crusts. *Earth and Planetary Science Letters*, *396*, 213–222. https://doi.org/10.1016/j.epsl.2014.04.021

Lockington, J. A., Cook, N. J., & Ciobanu, C. L. (2014). Trace and minor elements in sphalerite from metamorphosed sulphide deposits. *Mineralogy and Petrology*, *108*(6), 873–890. https://doi.org/10.1007/s00710-014-0346-2

Lorenzo, S. (1994). Structure and Stability of Cd surface complexes on ferric oxides. *Journal of Colloid and Interface Science*, *168*, 73–86.

McKenzie, R. (1980). The adsorption of lead and other heavy metals on oxides of manganese and iron. *Australian Journal of Soil Research*, 18(1), 61 - 73.

Michener, R., & Lajtha, K. (2008). Stable Isotopes in Ecology and Environmental Science: Second Edition. In *Stable Isotopes in Ecology and Environmental Science: Second Edition* (pp. 1–566). https://doi.org/10.1002/9780470691854

Mustafa, S., Waseem, M., Naeem, A., Shah, K. H., Ahmad, T., & Hussain, S. Y. (2010). Selective sorption of cadmium by mixed oxides of iron and silicon. *Chemical Engineering Journal*, *157*, 18–24. https://doi.org/10.1016/j.cej.2009.10.036

Ogata, F., Nagahashi, E., Miki, H., & Saenjum, C. (2020). Assessment of Cd (II) adsorption capability and mechanism from aqueous phase using virgin and calcined lignin. *Heliyon*, *6*(April), 252–294. https://doi.org/10.1016/j.heliyon.2020.e04298

Ohtaki, H. (1981). X-ray diffraction studies on the structures of cadmium iodide. *Pergamon Press*, *53*, 1357–1364

Pfennig, G. (1998). *Karlsruher Nuklidkarte Chart of the Nuclides.* Technik und Umweilt, Forschungszentrum Karlsruhe.

Rehk, M. (2013). Natural and Anthropogenic Cd Isotope Variations Natural and Anthropogenic Cd Isotope Variations. In M. Baskaran (Ed.), *Handbook of Environmental Isotope Geochemistry* (Issue December, pp. 125–153). Springer Heidelberg Dordrecht London New York. https://doi.org/10.1007/978-3-642-10637-8

Ruthven, D. M. (2008). Fundamentals of Adsorption Equilibrium and Kinetics in Microporous Solids. In *Adsorption and Diffusion* (Issue January 2006, pp. 1–43). Springer-Verlag Berlin Heidelberg. https://doi.org/10.1007/3829_007

Schwertmann, U., Cornell, R.M., 2000. *Iron Oxides in the Laboratory: Preparation and characterization*, second ed. Wiley-VCH Verlag GmbH, Weinheim.

Shanthi, P., Tamilarasan, G., Anitha, K., & Karthikeyan, S. (2014). Film and pore diffusion modelling for adsorption of reactive RED-4 onto stercula quadrifida seed shell waste as activated carbon. *Rasayan J. Chem*, *7*(3), 229–240.

Shiel, A. E. (2010). Evaluation of zinc, cadmium and lead isotope fractionation during smelting and refining. *Science of The Total Environment*, 408, 2357–2368.

Schimtt, A. D. (2009). High-precision cadmium stable isotope measurements by double spike thermal ionisation mass spectrometry. *Journal of Analytical Atomic Spectrometry*, 24(8), 1079-1088.

Schmitt, A. D., Galer, S. J., & Abouchami, W. (2009). Mass-dependent cadmium isotopic variations in nature with emphasis on the marine environment. *Earth and Planetary Science Letters*, *277*(1-2), 262-272.

Schmitt, A. D., Galer, S. J., & Abouchami, W. (2009). High-precision cadmium stable isotope measurements by double spike thermal ionisation mass spectrometry. *Journal of Analytical Atomic Spectrometry*, *24*(8), 1079-1088.

Simonin, J. (2016). On the comparison of pseudo-first order and pseudo-second order rate laws in the modeling of adsorption kinetics. *Chemical Engineering Journal*, *300*, 254–263. https://doi.org/10.1016/j.cej.2016.04.079

Smernik, R. (2003). Environmental Soil Chemistry. In *Agriculture, Ecosystems & Environment* (Vol. 100, Issue 1, pp. 94–95). https://doi.org/10.1016/s0167-8809(03)00222-6

Smith, K. S. (1999). Metal Sorption on Mineral Surfaces: An Overview with Examples Relating to Mineral Deposits. In *The Environmental Geochemistry of Mineral Deposits. Part B: Case Studies and Research Topics* (pp. 6, 161–180).

Sposito, G. (2008). *The Surface Chemistry of Natural Particles*. Oxford University Press, Oxford, UK.

Strawn, D. G., & Bohn, H. L. (2015). Adsorption Processes in Soils. In *Soil chemistry* (Forth edition, pp. 251–294). John Wiley & Sons, INC. https://ebookcentral-proquest-com.infozdroje.czu.cz

Tan, K. L., & Hameed, B. H. (2017). Insight into the adsorption kinetics models for the removal of contaminants from aqueous solutions. *Journal of the Taiwan Institute of Chemical Engineers*, *74*, 25–48. https://doi.org/10.1016/j.jtice.2017.01.024

Tiwari, M., Singh, A. K., & Sinha, D. K. (2015). Stable Isotopes: Tools for Understanding Past Climatic Conditions and Their Applications in Chemostratigraphy. In *Chemostratigraphy: Concepts, Techniques, and Applications* (pp. 65–92). Elsevier Inc. https://doi.org/10.1016/B978-0-12-419968-2.00003-0

Toner, B., Manceau, A., Webb, S. M., & Sposito, G. (2006). Zinc sorption to biogenic hexagonal-birnessite particles within a hydrated bacterial biofilm. *Chemical Geology*, *70*, 27–43. https://doi.org/10.1016/j.gca.2005.08.029

Vasconcelos, I. F., Haack, E. A., Maurice, P. A., & Bunker, B. A. (2008). EXAFS analysis of cadmium (II) adsorption to kaolinite. *Chemical Geology*, *249*, 237–249. https://doi.org/10.1016/j.chemgeo.2008.01.001

Violante, A., & Pigna, M. (2003). Adsorption of heavy metals on mixed Fe-Al oxides in the absence or presence of organic ligands. *Water, Air and Soil Pollution*, *145*, 289–306. https://doi.org/10.1023/A:1023662728675

Wang, J., & Guo, X. (2020). Chemosphere Adsorption isotherm models: Classification, physical meaning, application and solving method. *Chemosphere*, *258*, 127279. https://doi.org/10.1016/j.chemosphere.2020.127279

Wasylenki, L. E., Swihart, J. W., & Romaniello, S. J. (2014). Cadmium isotope fractionation during adsorption to Mn oxyhydroxide at low and high ionic strength. *Geochimica et Cosmochimica Acta*, *140*, 212–226. https://doi.org/10.1016/j.gca.2014.05.007

Wen, H. Z. (2015). Tracing sources of pollution in soils from the Jinding Pb-Zn mining district in China using cadmium and lead isotopes. *Applied Geochemistry*, 52, 147–154.

White, W. M. (2004). Chapter 9: Stable Isotope Geochemistry. In *Geochemistry* (pp. 361–420). https://doi.org/10.1002/chin.201229032

Wiederhold, J. G. (2015). Metal stable isotope signatures as tracers in environmental geochemistry. *Environmental Science and Technology*, *49*(5), 2606–2624. https://doi.org/10.1021/es504683e

Yong-Gui, C. (2011). Effect of contact time, pH, and ionic strength on Cd (II) adsorption from aqueous solution onto bentonite from Gaomiaozi, China. *Environmental Earth Sciences*, *64*(September), 329–336. https://doi.org/10.1007/s12665-010-0850-6

Zhu, C. W., Wen, H. J., Zhang, Y. X., Fan, H. F., Fu, S. H., Xu, J., & Qin, T. R. (2013). Characteristics of Cd isotopic compositions and their genetic significance in the lead-zinc deposits of SW China. *Science China Earth Sciences*, *56*(12), 2056–2065. https://doi.org/10.1007/s11430-013-4668-4